

10 **Abstract:** The Solnhofen pterosaurs *Pterodactylus antiquus*, *Aerodactylus*
11 *scolopaciceps*, *Diopecephalus kochi*, *Germanodactylus cristatus* and *Germanodactylus rhamphastinus*
12 all have complicated taxonomic histories. Species originally placed in the genus *Pterodactylus*, such
13 as *Aerodactylus scolopaciceps*, *Ardeadactylus longicollum*, *Cycnorhamphus suevicus* and
14 *Germanodactylus cristatus* possess apomorphies not observed in the type species of *Pterodactylus*,
15 and consequently have been placed in new genera. The affinities of another Solnhofen pterosaur
16 previously placed in *Pterodactylus*, *Diopecephalus kochi*, are less clear. It has been proposed that *D.*
17 *kochi* is a juvenile specimen of *Pterodactylus antiquus*, or perhaps “*Germanodactylus*
18 *rhamphastinus*” specimens are mature examples of *D. kochi*. Furthermore, studies have suggested
19 that “*Germanodactylus rhamphastinus*” is not congeneric with the type species of *Germanodactylus*.
20 Geometric morphometric analysis of prepubes and a cladistic analysis of the Pterosauria elucidate
21 plesiomorphic and apomorphic conditions for basal Jurassic pterodactyloids. *Germanodactylus* is
22 found to be a monotypic genus and *Pterodactylus*, *Diopecephalus*, and “*G. rhamphastinus*” are found
23 as distinct taxa belonging in individual genera, diagnosable using a combination of characters. Thus,
24 *Diopecephalus kochi* is not demonstrated to be congeneric with *Germanodactylus* or *Pterodactylus*
25 and is maintained as a valid taxon. “*G. rhamphastinus*” is readily distinguishable from other
26 Solnhofen pterosaur taxa, and a new genus is erected for its reception.

27

28 **Keywords:** Solnhofen, *Pterodactylus*, *Germanodactylus*, Phylogeny, Taxonomy, Cladistic analysis,
29 Geometric morphometrics

30 The Late Jurassic Franconia laminated limestone lagerstätten, typified by the Solnhofen Limestone,
31 Bavaria yield exceptionally well preserved vertebrate fossils, including pterosaurs. The pterosaurs
32 found in these laminated limestones are often fully articulated, with three-dimensional bones on
33 two-dimensional slabs, and sometimes preserve soft-tissues (e.g. Frey and Martill 2003). Presently,
34 there are eleven valid pterosaur genera, representing both monofenestratans and non-
35 monofenestratans. However, the biodiversity of the Late Jurassic Franconia laminated limestones
36 may be higher than previously thought, should those genera prove to be paraphyletic.

37 Until relatively recently, the genus *Pterodactylus* Cuvier, 1809 had been a wastebasket taxon that
38 has included many diverse pterosaurs, including some that are now recognized as basal non-
39 pterodactyloids. Throughout the 19th, 20th and 21st centuries, specimens were split from the type
40 species *Pterodactylus antiquus* (Sömmerring 1812) (BSP AS I 739) and placed in different genera and
41 families. Most recently, the wastebasket species *Pterodactylus kochi* (Wagner 1837) (BSP AS XIX 3
42 and SMF R 404) (Fig. 1) was reviewed and the majority of specimens assigned to the taxon were
43 reallocated to the species "*Pterodactylus scolopaciceps*" Meyer, 1860, for which the replacement
44 genus name *Aerodactylus* was erected (see Vidovic and Martill 2014). The remaining three
45 specimens under the name *Pterodactylus kochi* require a review, to establish if they comprise a
46 unique species in the genus, or if they are juveniles of *Pterodactylus antiquus*, or indeed, a juvenile
47 of any other Tithonian pterosaur. Vidovic and Martill (2014) hypothesised that "*P. kochi*" was a
48 juvenile of "*Germanodactylus rhamphastinus*" (Wagner 1851) (BSP AS I 745 a and b) (Fig. 2) and that
49 both might belong to the genus *Diopecephalus* Seeley, 1871, for which *Diopecephalus kochi* is the
50 type species. Indeed, the placement of "*G. rhamphastinus*" in the genus *Germanodactylus* Young,
51 1964 has been called into question in the past (Maisch et al. 2004; Wang et al. 2008), but no
52 appropriate taxonomic action was taken. Here, a taxonomic review of "*Pterodactylus kochi*" and
53 "*Germanodactylus rhamphastinus*" is presented. The specimens are placed in geological context,
54 compared anatomically, a geometric morphometric analysis is used to test the validity of
55 morphological observations, and a cladistic analysis is performed to test the monophyly of the
56 genera *Pterodactylus* and *Germanodactylus*.

57 **Institutional abbreviations**

58 BMMS, Museum Solnhofen (formerly: Bürgermeister Müller Museum, Solnhofen); BSP, Bayerische
59 Staatssammlung für Paläontologie Munich; JME, Jura Museum, Eichstätt; NHMUK, Natural History
60 Museum, London; NMING, National Museum of Ireland, Dublin; OUMNH, Oxford University Museum
61 of Natural History; PTH, Philosophisch-Theologische Hochschule, Eichstätt (Jura Museum); SMF,

62 Senckenberg Museum, Frankfurt; SMNK, Staatliches Museum für Naturkunde Karlsruhe; SMNS,
63 Staatliches Museum für Naturkunde Stuttgart.

64 **Taxonomic review**

65 *On "P. kochi": Diopecephalus and Aerodactylus*

66 Using multiple lines of evidence, Vidovic and Martill (2014) demonstrated that "*P. kochi*" (*sensu*
67 Wellnhofer 1968, 1970; Jouve 2004; Bennett 2013a) was a wastebasket taxon. Historically, sub-adult
68 specimens were included in the taxon due to size criteria and convergent morphology in early
69 ontogeny (Vidovic and Martill 2014). A subset of specimens referred to "*P. kochi*" shared common
70 cranial, vertebral and pteroid characters that were distinct from the holotype of the species. The
71 specimens belonging to this distinct morphotype consistently plot separately from specimens more
72 similar to the holotype of "*P. kochi*" in morphometric bivariate plots (Vidovic and Martill 2014:
73 Supporting Information S2.1). One specimen (BSP AS V 29 a/b) plotting as the distinct morphotype is
74 a species name bearer with date priority, a new genus was erected for its reception (Vidovic and
75 Martill 2014), producing the new combination *Aerodactylus scolopaciceps* (Meyer 1860). The
76 detection of *Aerodactylus* specimens referred to "*P. kochi*" does not mean that the latter taxon is
77 not a junior subjective synonym of *P. antiquus* (*sensu* Jouve 2004; Bennett 2013a). However, the two
78 *Pterodactylus* species were demonstrated to be morphometrically distinct (Vidovic and Martill 2014:
79 Supporting Information S2.1) and were found to be paraphyletic in cladistic analyses of the
80 Pterodactyloidea (Howse 1986; Lü and Ji 2006; Lü et al. 2006; Lü 2009; Vidovic and Martill 2014).
81 From this point forward, for clarity and to promote taxonomic stability, the full binomial
82 *Diopecephalus kochi* is used rather than "*Pterodactylus kochi*", except in historical context.

83 *Diopecephalus: type species*

84 The holotype of "*Pterodactylus kochi*" was considered to belong to a distinct genus by Seeley (1871),
85 which he unambiguously named *Diopecephalus* Seeley, 1871. Seeley (1871) also included
86 "*Pterodactylus longicollum*" Meyer, 1854 and "*Pterodactylus rhamphastinus*" (Wagner, 1851) in the
87 genus *Diopecephalus*. Bennett (2006, 2013a) discussed this at length, but perhaps due to a small
88 grammatical error on Seeley's part, argued that Seeley did not designate a type species for
89 *Diopecephalus* until 20 years later (Seeley 1901). However, Seeley (1871) did put the other two
90 "*Pterodactylus* spp." 'under the name *P. kochi*' in the genus *Diopecephalus*, thus erecting a polytypic
91 *Diopecephalus*:

92 'Another unnamed generic type is typified by *Pterodactylus longicollum*, *P. rhamphastinus*, and the
93 two species' ... are... 'included under the name *P. kochi*. In this genus the middle hole of the skull is
94 entirely wanting. For it I suggest the name *Diopecephalus*.' Seeley 1871: p.35

95 On "*P. longicollum*"

96 It is noteworthy that Seeley (1871, 1901) was referring to the holotype of "*P. longicollum*", which he
97 would have seen a cast of in the Natural History Museum, London (NHMUK R 37990), not the
98 original material that was later destroyed during WWII. Wellnhofer (1970) elected a neotype (SMNS
99 56603) for "*P. longicollum*" using a specimen originally described by Plieninger (1907) from a slightly
100 older formation and different locality compared to the original. Finding SMNS 56603 to be distinct
101 from *Pterodactylus*, Bennett (2013a) erected the new genus *Ardeadactylus* for its reception, an
102 action with which we are in full agreement. Although we do not necessarily agree that SMNS 56603
103 is conspecific with Meyer's (1854) "*Pterodactylus longicollum*". The ulnae and radii were not
104 preserved in the holotype, thus it is impossible to interpret wing proportions and it may represent
105 any aurorazhdarchian with the exception of *Cycnorhamphus* Seeley, 1870 which has unambiguous
106 cranial autapomorphies.

107 On "*G. rhamphastinus*"

108 The remaining taxon within Seeley's (1871) *Diopcecephalus* hypodigm is "*Germanodactylus*
109 *rhamphastinus*" (Fig. 2). There are currently three specimens identified as "*G. rhamphastinus*"
110 (Wellnhofer 1968; Bennett 2002; Rodrigues et al. 2010). Each specimen possesses a straight rostrum
111 terminating in a point. The skull is relatively deep when compared to other Jurassic pterodactyloids
112 and the cervical vertebrae are shorter. "*Germanodactylus rhamphastinus*" has a complex taxonomic
113 history which has been examined on several occasions recently (Bennett 1996, 2002, 2006; Maisch
114 et al. 2004; Wang et al. 2008; Rodrigues et al. 2010; Vidovic and Martill 2014).

115 Many phylogenetic studies demonstrate that the two species of *Germanodactylus* nest together
116 (Kellner 2003; Unwin 2003; Andres and Ji 2008; Lü et al. 2009; Wang et al. 2009; Andres et al. 2014)
117 in a monophyletic clade, but a more focussed analysis by Maisch et al. (2004) demonstrates the
118 genus to be paraphyletic. Maisch et al. (2004) created the *nomen nudum* *Daitingopterus*, intended
119 for the reception of "*G. rhamphastinus*" by placing the name in a table with no specific reference to
120 a specimen. Subsequently, Wang et al. (2008) noted that the tooth morphology of "*G.*
121 *rhamphastinus*" (Fig. 2) differs from that of *Germanodactylus cristatus* (Wiman 1925) (BSP 1892 IV 1
122 and NMING F15005) (Fig. 3) and suggested that the former may be placed in a new genus, but still
123 closely related to *Germanodactylus*. Rodrigues et al. (2010) reiterated that "*G. rhamphastinus*"
124 might be generically distinct from *G. cristatus*. In a more comprehensive cladistic analysis of
125 pterodactyloids Vidovic and Martill (2014) found Archaeopterodactyloidea of Kellner (2003) and
126 Dsungaripteroidea of Unwin (2003) to be polyphyletic. Vidovic and Martill (2014) recovered
127 *Germanodactylus cristatus* as a basal tapejaroid, while "*G. rhamphastinus*" was recovered as a basal

128 “transitional” taxon close to Aurorazhdarchidae. Furthermore, when the data of the Lü et al. (2009)
129 analysis is re-run using TNT with *Noriopterus* Young, 1973 included (as it was in the published matrix),
130 a significantly shorter tree than the published tree (lacking *Noriopterus*) also finds *Germanodactylus*
131 to be paraphyletic.

132 The taxonomy of *Germanodactylus* and its present constituent species has most recently been
133 reviewed in detail by Bennett (2006). The type specimen, *G. cristatus* (BSP 1892 IV 1) was originally
134 described by Plieninger (1901) and identified as an example of “*P. kochi*”. But Wiman (1925)
135 considered BSP 1892 IV 1 distinct from “*P. kochi*” on account of its edentulous jaw tips and
136 prominent sagittal crest, thus he named it *Pterodactylus cristatus* Wiman, 1925 (Fig. 3). Young (1964)
137 considered BSP 1892 IV 1 to be generically distinct from *Pterodactylus* and erected the genus
138 *Germanodactylus*, making the combination “*G. kochi*” (Wagner 1837). As Bennett (2006) noted,
139 Young (1964) seemed unaware that this specimen had been renamed “*P. cristatus*” by Wiman
140 (1925). Wellnhofer (1968), aware of Wiman’s work, corrected Young’s *lapsus*, creating the binomial
141 *Germanodactylus cristatus* (Wiman 1925). Later, Bennett (2006) referred two specimens that had
142 previously been referred to “*P. kochi*” (JME SoS 4593) and “*Pterodactylus micronyx*” Meyer, 1856
143 (JME SoS 4006) to *Germanodactylus cristatus*, considering them to represent juveniles of that taxon.
144 In addition to these referrals, Bennett (2006) emended the diagnosis of *Germanodactylus* to
145 accommodate perceived ontogenetic changes and maintained “*G. rhamphastinus*” within the genus
146 contrary to Maisch et al. (2004).

147 Bennett’s (2006) revised diagnosis of *Germanodactylus* lacks autapomorphies and distinguishes
148 *Germanodactylus* from other pterosaurs by a combination of characters which are also possessed by
149 more basal and derived taxa. However, *Germanodactylus cristatus* (Fig. 3), the type species of
150 *Germanodactylus*, possesses autapomorphies not found in “*G. rhamphastinus*” (Fig. 2) such as
151 edentulous jaw tips. Thus, *Germanodactylus* is rendered a metataxon. Here, “metataxon” is not used
152 in the strict phylogenetic sense (Archibald 1994) because its use is not in reference to a cladogram,
153 but because the taxon diagnosis cannot provide positive evidence of monophyly or paraphyly.
154 Consequently, here the diagnosis of *Germanodactylus* is emended, and “*G. rhamphastinus*” is
155 excluded from the genus.

156 Such an action, however, requires a reappraisal of the relationships of “*G. rhamphastinus*”. It is
157 difficult to distinguish “*G. rhamphastinus*” (Fig. 2) from the holotype of *Diopecephalus kochi* (Fig. 1)
158 other than by using size related criteria. While it is difficult to distinguish sub-mature specimens
159 from mature specimens, the only cladistic analyses known to include the holotype of *Diopecephalus*
160 *kochi* (Howse 1986; Vidovic and Martill 2014) (i.e. not *Aerodactylus* specimens) find *Pterodactylus*

161 spp. (including *D. kochi*) and *Germanodactylus* spp. paraphyletic. Here, a rigorous and
162 comprehensive cladistic analysis tests the relationship between “*G. rhamphastinus*”, *D. kochi*, *P.*
163 *antiquus* and *G. cristatus*. Appropriate taxonomic action is taken as a consequence of the outcome
164 of the analysis.

165 **Stratigraphic review**

166 The traditional subdivisions of the Franconia laminated limestones represent short periods of
167 geological time (<4 mya total duration: Late Kimmeridgian–Early Tithonian). Monofenestratan
168 pterosaurs are known from Malm Zeta 1–3 (Kimmeridgian–Tithonian) (Table 1.) from quarries near
169 Nusplingen, Solnhofen, Eichstätt, Schernfeld, Mörnshheim, Daiting, Schamhaupten, Painten, Kelheim
170 and Zandt in southern Germany. With the exception of *Pterodactylus* and possibly *Cycnorhamphus*
171 and *Ardeadactylus*, the vast majority of pterosaurs are restricted to single sub-divisions of the
172 Franconia laminated limestones, even when they are represented by many specimens.

173 Specimens of *Pterodactylus antiquus* are known from the Lower Tithonian, Malm Zeta 2 and 3
174 (Bennett, 2013a). The taxon may also be present in the earliest Tithonian (Malm Zeta 1) cropping out
175 at Zandt, Germany (SMF R 4072). *Diopecephalus kochi* and “*G. rhamphastinus*” are known only from
176 Malm Zeta 3, Lower Tithonian of Kelheim and Daiting respectively according to Wellnhofer (1970).
177 Exposures at Daiting are in the Moernsheimensis Horizon and Subzone of the Hybonotum Zone,
178 making it the youngest pterosaur-bearing strata in the Franconia limestones (Schweigert 2007).
179 Kelheim is reportedly in the Rueppelliansus Subzone of the Hybonotum Zone (Schweigert 2007),
180 making it equivalent to Malm Zeta 2. The *Diopecephalus* locality is ~1 km North of Kelheim
181 (Wellnhofer 1970), close to Painten (~6 km) which is Malm Zeta 1. Therefore, the age of
182 *Diopecephalus* according to Wellnhofer (1970) (Malm Zeta 3) is in some doubt. Although the
183 “Papierschiefer” has been considered contemporary with Mörnshheim Limestone (Meyer 1977),
184 crushed *Gravesia gigas* (*riedlingensis* subzone) ammonites were misidentified as *G. gravesiana*
185 resulting in a younger date being determined (Schweigert 2007). *Germanodactylus cristatus* is
186 known from two juvenile and two mature specimens, of which the holotype (BSP 1892 IV 1 and
187 NMING F15005) is from Eichstätt, Malm Zeta 2, Lower Tithonian.

188 The Painten pro-pterodactyloid (Tischlinger and Frey 2013) is from the Upper Kimmeridgian. The
189 specimen seemingly represents a late surviving transitional morphology between wukongopterids
190 and pterodactyloids. *Cycnorhamphus suevicus* (Quenstedt 1855) ranges from the Upper
191 Kimmeridgian to Lower Tithonian. A specimen referred to *Cycnorhamphus*, the now lost
192 “*Pterodactylus eurychirus*” Wagner, 1858 (Wellnhofer 1970) from Malm Zeta 2 is undiagnostic and

193 while it could represent *Cycnorhamphus* in Eichstätt, it could also represent an example of
194 *Ardeadactylus* or *Aurorazhdarcho*. However, *Cycnorhamphus* is known from the Lower Tithonian of
195 South-East France (Fabre 1976). The neotype of *Ardeadactylus longicollum* (Wellnhofer 1970) is from
196 Malm Zeta 1, Upper Kimmeridgian. The lost holotype is from the Lower Tithonian, Malm Zeta 2, but
197 as noted above it may not be conspecific with the neotype. Wellnhofer (1970) also referred other
198 lost specimens to this species, but they also lack diagnostic features. Notably, a specimen referred to
199 *Ardeadactylus*, "*Pterodactylus vulturinus*" Wagner, 1858 (Wellnhofer 1970) is an undiagnostic
200 isolated wing-metacarpal from Malm Zeta 3.

201 *Gnathosaurus subulatus* Meyer, 1834 and its sister taxon *Ctenochasma elegans* (Wagner 1861a) are
202 only known from Malm Zeta 2, Lower Tithonian. *Aurorazhdarcho micronyx* (Meyer 1856) is known
203 from juvenile specimens and an adult missing its skull (Frey et al. 2011) which are all from Malm Zeta
204 2. *Aerodactylus scolopaciceps* (Meyer 1860) is also known only from Malm Zeta 2 of Solnhofen and
205 Eichstätt, where the species is represented mostly by juvenile specimens. Additionally, a large wing
206 of an adult *Aerodactylus* with ~2.5 meter wingspan (figured by Wellnhofer 1970: Exemplar Nr 78)
207 (PTH 1963. 1 a) was found in Schernfeld, near Eichstätt (Malm Zeta 2).

208 *Stratigraphy of putative Diopecephalus kochi specimens*

209 A specimen referred to "*Pterodactylus kochi*" in the Oxford University Museum of Natural History
210 (OUMNH JZ 1609) and its counterpart in the Natural History Museum, London (NHM) (NHM UK PV R
211 3949) are labeled as coming from Solnhofen, Kimmeridgian. However, it is likely that precise locality
212 information was lost before the specimens were purchased for the museums (see supplementary
213 material S.3.1.1.).

214 Another specimen referred to "*Pterodactylus kochi*" (Wellnhofer, 1970: Exemplar Nr. 12) (SMF R
215 4072) by von Huene (1951) is noted to be from Zandt, Germany. This locality is lesser known for its
216 pterosaurs and is east of Kelheim and Painten, close to the Czech Republic. Stratigraphically, the
217 Zandt lagerstätte is from the lower Hybonotum Zone, contemporaneous with the youngest
218 lithographic limestone cropping out at Painten (Malm Zeta 1: earliest Tithonian) (Schweigert 2007).
219 The specimen's juvenile state makes it difficult to refer it to any one of the Jurassic German
220 pterosaurs that have a dentition extending from the jaw tips to a point under the nasoantorbital
221 fenestra (Vidovic and Martill 2014, fig. 3). However, what is visible of the prepubis is elongate and
222 narrow compared to *Diopecephalus* and "*G. rhamphastinus*". Additionally, the pedal and manual
223 unguals of this specimen are more robust than those of *Diopecephalus kochi* and "*Germanodactylus*
224 *rhamphastinus*", but similar to those of *Pterodactylus*.

225 Finally, An undescribed, privately owned specimen from Painten (Malm Zeta 1, Upper Kimmeridgian-
226 –Lower Tithonian) on display in the Museum Solnhofen is identified as “*Pterodactylus c.f. kochi*”
227 (Arratia et al. 2015: p.468). The morphology of this specimen most closely matches *Diopecephalus*
228 *kochi* and we agree with this assignation.

229 **Materials and methods**

230 *Cladistic analysis and appraisal*

231 A cladistic analysis of the Pterosauria, including all the taxa discussed here was performed. The
232 analysis included 104 operational taxonomic units (OTUs) comprising 99 pterosaurs and 5
233 archosauriforms as an outgroup. The taxa were coded for 320 characters, of which 44 have
234 continuous states and 276 have discrete states. Many of the characters are similar to those
235 previously published, but 249 of the characters in this analysis were developed independent of the
236 literature for an as of yet unpublished “distinct” analysis devised to test cladistic methods and clade
237 recovery in the Pterosauria. The additional 71 characters were taken or modified from the literature.
238 Great care was taken to avoid compound characters (Brazeau 2011) or combining multiple states
239 into one. Martill et al. (2016) have demonstrated the benefits of this practice.

240 The analysis was performed in TNT using a “new technology search” (NT) (Goloboff et al. 2008a) and
241 a “traditional search” was run, swapping from the saved NT trees, to find the maximum number of
242 most parsimonious trees (MPTs). In the Vidovic and Martill (2014) analysis, four of the continuous
243 characters required rescaling with the equation $i = \tan^{-1}a/b$, where i is the index number analysed
244 and a/b is the quotient value of the elements being studied. Mongiardino Koch et al. (2015)
245 subsequently suggested logarithmically transforming the quotient values for continuous states, to
246 avoid the problems of researchers deciding to use either “top heavy” or “bottom heavy”
247 dividend/divisor relationships. However, both of these methods produce a continuum of weighted
248 states that are an exponential function of the morphometric data. In this analysis, the characters
249 were simply transformed using “top heavy” quotients. Where converse data was present in a
250 character’s coding, the equation was inverted to make it “top heavy” and made negative to
251 differentiate it from those states that were not the product of an inverted equation. To ensure that
252 the continuum of data was evenly spaced according to the morphological variation, the negative
253 numbers had 1 added to them and positive numbers had 1 subtracted. A normalization equation
254 was then used to transform negative numbers into positive numbers and place the data range
255 between 0 and 3. Performing this data transformation rather than the trigonometric one (Vidovic
256 and Martill 2014), or the logarithmic one (Mongiardino Koch et al. 2015), results in a continuum of

257 weighted states that are a direct function of the morphometric data, while resolving the problem of
258 converse data and researcher decision. A manuscript detailing the advantages of this method of
259 continuous data transformation over the previous one used by these authors (Vidovic and Martill
260 2014) is in preparation. Three (3.000) was chosen as the number of continuous states, rather than
261 1.000, as in Andres et al. (2014) and Vidovic and Martill (2014) or 2.000 as employed by (Pereyra and
262 Mound 2009). The reason for choosing 3.000 states for continuous characters is that during trial and
263 error experiments it produces a similar distribution of character reversals (plotted in a frequency
264 histogram) compared to the discrete state characters, showing that the analysis was not biased
265 towards any one type of character.

266 Implied weights were used during the analysis to weight against homoplasy (Goloboff et al. 2008b;
267 Goloboff 2014). Using implied weighting means the researcher makes the least assumptions out of
268 any weighting method – even using equal weights assumes that all characters are equally
269 informative. However, the implied weighting method requires a concavity constant (K) and no
270 consensus for which number should be used has been reached in the literature. It is possible to
271 reverse the equation ($W = \frac{[-K] + [K+es]}{[K+es]}$, where W is the weight and es is the extra steps) in
272 order to calculate the K value required to transform a character with a designated fit into a
273 predetermined weight. However, this method requires a researcher to decide *a priori* what
274 character fit is excessively homoplastic and the weight this homoplastic character should receive.
275 Experimentation with different K values, plotting fit against the implied weight demonstrates that
276 the higher the number, the more linear the relationship becomes, whereas lower K values produce
277 exponential curves. The TNT default K value of 3 approximates a logarithmic curve, meaning that
278 poorer fitting characters are increasingly weighted against. Because of this “smooth” curvilinear
279 relationship between fit and weight, 3 is selected as the optimal K value for this analysis.

280 The outgroup (*Erythrosuchus*, *Euparkeria*, *Scleromochlus*, *Lagerpeton*, and *Marasuchus*) is distinct
281 among pterosaur analyses, but similar to the outgroups of some dinosaur analyses (Nesbitt et al.
282 2009). There were multiple reasons for altering the outgroup; 1) the combination of multiple taxa
283 into a single hypothetical outgroup (Unwin 2003) is not a sound basis for polarizing characters or
284 testing the ingroup’s monophyly; 2) the use of derived pseudosuchians and dinosaurs increased the
285 opportunity for homoplasy, especially in the ankle (Bennett 2013b); 3) different authors use
286 different outgroups, possibly polarizing characters differently. Polarizing characters biased towards
287 the method of a single authorship could result in similar results due to shared methodology.
288 Alternatively, multiple rooting methods could have been used, but it is difficult to estimate the
289 composite outgroup of Unwin (2003) based on an almost entirely distinct character list.

290 The resulting tree was plotted on a geological time scale using the statistics program R and the
 291 packages phytools (Revell 2012) and strap (Bell and Lloyd 2014). The online Paleobiology Database
 292 (<http://fossilworks.org>) was used to place the taxa stratigraphically. Using the chronostratigraphic
 293 tree it is possible to calculate the gap excess ratio (GER) (Wills 1999) to correlate the phylogenetic
 294 results with the fossil record.

295 To compare the cladogram to key analyses (Maisch et al. 2004; Lü et al. 2009; Wang et al. 2009;
 296 Andres et al. 2014) the taxon lists were reduced to common taxa only, using CompPhy (Fiorini et al.
 297 2014). The SPR distances (Goloboff 2008) and Robinson-Foulds distances (R-F) (Robinson and Foulds
 298 1981) were calculated using TNT and CompPhy. A new index termed the clade retention index (CRI)
 299 was calculated using the Phytools package in R. An R script was written to implement the equation
 300 given below, and it is available in the supplementary material. Like the consistency fork index (CFI)
 301 (Colless 1980) the CRI uses a consensus of two trees to calculate tree similarity. Unlike the CFI, the
 302 CRI considers the polytomous taxa (not clades in polytomies) in the strict consensus, indicating how
 303 many monophyletic clades are shared between cladograms.

304 The CRI is calculated using the equation below, where nodes (N) on the consensus tree are
 305 indicators of agreement and individual taxa in polytomies (P) are an indicator of disagreement. To
 306 put the information about clade retention into context, the maximum possible agreement is
 307 calculated using the number of common taxa (T) minus one. The maximum index number (i)
 308 recoverable is 1 and the minimum is -1, so the result can be range scaled (normalized) to give a CRI
 309 between naught and one ($X = 1$), see equations below.

310

$$i = -\frac{P - N}{T - 1}$$

$$\therefore CRI = \frac{X}{(Rmax - Rmin) \times (i - Rmin)}$$

$$\therefore CRI = \frac{1}{(1 - -1) \times \left(-\frac{P - N}{T - 1}\right) - -1}$$

$$\therefore CRI = 0.5 \times \left(-\frac{P - N}{T - 1}\right) + 1$$

311 The reason for using three different tree comparison metrics is that no one metric represents all the
 312 information available. Additionally, tree comparison metrics can be confounded and should be used

313 in tandem. For example, the CRI will produce deflated similarity values if the trees being compared
314 already have polytomies. Also, the SPR metric can assign two different sets of trees with different
315 levels of agreement the same score.

316 Tanglegrams can be helpful for interpreting the results of tree comparison metrics. Dendextend
317 (Galili 2015) in R was used to produce tanglegrams of the reduced taxon trees produced by
318 CompPhy. In order to perform the analysis that produces a tanglegram in Dendextend, the
319 polytomies had to be randomly resolved. To provide as much information about tree similarity as
320 possible solid lines are used to represent branches that are agreed upon, dashed lines represent
321 unique branches, and the lines between the tree tips tangle to represent the disagreement after the
322 branches are rotated for maximum fit.

323 *Geometric morphometrics*

324 The prepubis of *Germanodactylus cristatus* is morphologically distinct from that of *G.*
325 *rhamphastinus*, which has a morphology more similar to that of *Diopecephalus* and *Darwinopterus*.
326 Descriptions and discussions of the prepubis morphology are lacking in the literature. Here, the
327 hypothesis that the morphology and proportions of this often overlooked bone are taxonomically
328 informative is tested using geometric morphometrics. Furthermore, it is hypothesised that *D. kochi*,
329 *D. modularis*, and "*G. rhamphastinus*" are more similar than any one is to *P. antiquus*.

330 The geometric morphometric analysis is compared with the phylogeny to establish if their
331 morphology can be used for taxonomic purposes. The analysis was performed on standardised
332 bitmap outline drawings of prepubes. The outlines were drawn from referred specimens of
333 *Dorygnathus* Wagner, 1860 (Wyoming Dinosaur Center specimen); *Scaphognathus* Wagner, 1861b
334 (SMNS 59395); *Darwinopterus* Lü et al., 2009 (41HIII-0309A); *Aerodactylus* Vidovic and Martill, 2014
335 (BSP 1883 XVI 1); *Ctenochasma* Meyer, 1852 (BSP 1935 I 24) and "*G. rhamphastinus*" (JME Moe 12 &
336 BSP 1977 XIX 1), and the holotypes of *Pterodactylus antiquus*; *Diopecephalus kochi*;
337 *Germanodactylus cristatus* and *Cycnorhamphus suevicus*. In some cases, it was necessary to use the
338 part and counterpart or moulds of the bone in the limestone to reconstruct the entire prepubis
339 morphology. In *Pterodactylus* a portion of the distal expansion is overlaid by the femur, so a
340 conservative estimate was made of the outline. The shapes were digitized by selecting a net of 100
341 landmarks in TSPdig 2 (Rohlf 2010). The TPS file was analysed in R using the package Geomorph
342 (Adams and Otárola-Castillo 2013). A generalized Procrustes analysis was performed, projecting the
343 landmark data into linear tangent space. The x-axis of the resulting principal component analysis was

344 converted into hierarchical clusters which were then plotted as a radial dendrogram (note the y-axis
345 produces the same results).

346 **Results**

347 *Cladistics*

348 The cladogram presented here is a strict consensus of 2 most parsimonious trees (Fig. 4), which is
349 highly congruent with the geological record (GER = 0.902). The cladogram demonstrates a
350 paraphyletic “rhamphorhynchoidea” with a sister group of *Preondactylus* Wild, 1983 and
351 *Austriadactylus* Dalla Vecchia et al., 2002 as the most basal branch of Pterosauria. This result is in
352 broad agreement with Unwin (2003), Dalla Vecchia (2009), Lü et al. (2009) and Andres et al. (2014).
353 Those Triassic pterosaurs possessing laterally compressed lanceolate or triangular teeth with coronal
354 serrations are recovered in a monophyletic clade, distinct from those with multiple cusps. Multi-
355 cusped taxa share a common ancestor with all remaining taxa with single-cusped teeth. Only the
356 taxa with single-cusped teeth, lacking serrations survived the end-Triassic extinction. Although
357 *Dorygnathus* and *Campylognathoides* are not found until the Toarcian, their shared common
358 ancestor with *Dimorphodon* Owen, 1859 must have been a Triassic pterosaur.

359 Scaphognathidae contains an assortment of taxa with well-spaced, simple conical teeth, a convex
360 dorsal margin to the skull, a slender dorsal process of the maxilla, a large round orbit, a low angle of
361 the jaw symphysis to the ramus, a robust bowed pteroid bone, a reduced ventral crest of the wing
362 metacarpal and distal phalanx of pedal digit 4 that is longer than the preceding phalanges. These
363 uniting characters place anurognathids (reclassified here to Anurognathinae) in Scaphognathidae.
364 Their deeply nested placement within Scaphognathidae is likely to be due to a lack of transitional-
365 morphs combined with their paedomorphism. Thus, it is possible that anurognathines are far more
366 basal members of Scaphognathidae and the analysis was confounded by their aberrant morphology.
367 The paedomorphic characters exhibited by anurognathines (e.g. reduced rostrum length, large orbit,
368 deep skull, shorter caudal vertebrae) might be the reason some researchers (e.g. Kellner 2003; Wang
369 et al. 2009) find them as the most basal taxa in Pterosauria.

370 *Parapsicephalus* Arthaber, 1919 is closely related to scaphognathids, but it maintains some
371 plesiomorphic characteristics which in the past have led to it being likened to *Dorygnathus*
372 (Carpenter et al. 2003; Unwin 2003) and *Dimorphodon* (Andres et al. 2014). In this analysis, however,
373 *Parapsicephalus* is the sister taxon to Monofenestrata (Lü et al. 2009).

374 Monofenestrata comprises two non-pterodactyloid clades and Pterodactyloidea. Wukongopteridae
375 contains *Wukongopterus* Wang et al., 2009, *Darwinopterus* spp., and *Changchengopterus* Lü, 2009. It

376 may be that many wukongopterids comprise a single genus for which *Changchengopterus* has
377 priority. The results of this analysis demonstrate that wukongopterids are in desperate need of a
378 taxonomic review less than a decade after their discovery, in agreement with Sullivan et al. (2014).
379 The next taxon stepwise is the as yet un-named German monofenestratan dubbed the Painten pro-
380 pterodactyloid (Tischlinger and Frey 2013). The specimen exhibits a long 5th toe and a shortened tail
381 with elongate chevrons, otherwise, it is *Pterodactylus*-like. *Eosipterus* and *Pterodactylus* are found to
382 be the most basal members of Pterodactyloidea due to the extreme reduction of the 5th toe and
383 reduced tail lacking elongate chevrons. Similar to Vidovic and Martill (2014), this analysis finds
384 *Pterodactylus* to be a very basal member of Pterodactyloidea excluded from the monophyletic clade
385 containing *Ctenochasma* and *Cycnorhamphus* where it has been found by many analyses (Kellner
386 2003; Unwin 2003; Andres et al. 2014). Despite the lack of consensus on the placement of
387 *Pterodactylus*, its placement here is consistent with recent discoveries of non-pterodactyloid
388 monofenestratans. Likewise, the paraphyly of Archaeopterodactyloidea and *Germanodactylus* is
389 consistent with the discovery of the wukongopterids and *Hamipterus* Wang et al., 2014, meaning
390 characters that were previously thought to be synapomorphies for these clades are in fact
391 symplesiomorphies, and synapomorphies of Monofenestrata. The basal position of *Pterodactylus*
392 excludes it from Lophocratia, which is divided into Euctenochasmatia and Eupterodactyloidea. The
393 most recent definition of Eupterodactyloidea (Andres et al. 2014) does not define a clade similar to
394 the one proposed by Bennett (1994) on this tree, so it is redefined here as the most inclusive clade
395 containing *Nyctosaurus* Marsh, 1876a, *Pteranodon* Marsh, 1876b, *Dsungaripterus* Young, 1964 and
396 *Azhdarcho* Nesov, 1984 (after Bennett 1994), but not *Pterodaustro* Bonaparte, 1970.

397 *Diopecephalus* is the most basal member of a monophyletic clade containing *Pterodaustro* and
398 *Cycnorhamphus*, thus Euctenochasmatia contains Ctenochasmatoidea (Unwin 2003).
399 Ctenochasmatoidea further contains Ctenochasmatidae and Aurorazhdarchia. Here,
400 Aurorazhdarchidae is redefined as pterosaurs closer to *Aurorazhdarcho* than they are to
401 *Cycnorhamphus*. The name Aurorazhdarchia is used as the unranked replacement name for the
402 clade originally defined as Aurorazhdarchidae (Vidovic and Martill 2014), and it comprises
403 *Aerodactylus*, Aurorazhdarchidae, and Gallodactylidae.

404 "*Germanodactylus rhamphastinus*" is found to be the most basal branch of Eupterodactyloidea,
405 followed stepwise by *Germanodactylus cristatus* and *Elanodactylus* Andres and Ji, 2008.

406 *Elanodactylus* is the sister taxon to Dsungaripteroidea *sensu* Kellner (2003), but Young (1964)
407 considered Dsungaripteroidea to be defined as pterosaurs with a notarium, in which case
408 *Germanodactylus cristatus* is the most basal dsungaripteroid. Indeed, in addition to other

409 synapomorphies, the presence of a notarium defines the clade (Dsungaripteroidea) comprising
410 *Germanodactylus*, *Quetzalcoatlus* Lawson, 1975 and *Nyctosaurus*.

411 The subjects of this study represent the most basal members of Pterodactyloidea and Lophocratia,
412 excluded from the derived monophyletic clade Ctenochasmatoidea. *Diopecephalus*, a basal most
413 member of Lophocratia is found to possess characters placing it in the monophyletic clade
414 Euctenochasmata, while "*G. rhamphastinus*" and *G. cristatus* are found to possess characters of
415 Eupterodactyloidea. whereas, *Pterodactylus* is found more basal than any of the other Franconia
416 laminated limestone pterodactyls. Given that the holotype of the type and only species is a
417 mature subadult and nearly complete, it is not expected to have suffered "rootward slippage" during
418 the analysis.

419 The taphonomic state of *Diopecephalus* may have caused "cladeward slippage" or "rootward
420 slippage", as modular evolution in pterosaurs has been demonstrated to cause both (Lü et al. 2009)
421 due to derived or plesiomorphic states being present in distinct morphological units which can be
422 lost during fossilisation. Two of the discrete state characters that place *Diopecephalus* in
423 Euctenochasmata (characters 104 and 248) are difficult to code due to its small size and variable
424 state of preservation across the slabs. To test for "cladeward slippage" the two characters were
425 made inactive and the analysis was re-run. This analysis did result in *Diopecephalus* slipping
426 rootward by one branch, out of the monophyletic Euctenochasmata, but it was still not found in a
427 monophyletic clade with *Pterodactylus* or "*G. rhamphastinus*".

428 The comparison metrics (Fig. 5–7) demonstrate good agreement between the three phylogenies
429 with a paraphyletic *Germanodactylus* (Maisch et al. 2004; Lü et al. 2009). Although the tanglegrams
430 (Fig. 8) demonstrate that similarity metrics (Fig. 5–7) are not independent of matrix dimensions.
431 Smaller trees have less opportunity to be incongruent, but fewer unique relationships are required
432 to lower the congruence metric significantly. To clarify the relationships of "*Germanodactylus*" spp.
433 the phylogeny presented here and the phylogeny of Lü et al. (2009) (Fig. 8 cii) were pruned to their
434 taxa common with Maisch et al. (2004) (Fig. 8 ci). The pruned trees compare favourably despite the
435 lack of topological congruence in the rest of the tree.

436 The CRI (Fig. 5) produces comparable results to the R-F distance metric (Fig. 6), demonstrating its
437 utility. However, the CRI has been affected by the polytomies already present in the source trees.
438 Most noticeably, values from the comparisons of the Lü et al. (2009) phylogeny are lowered by
439 polytomies that are already present in the source tree. By comparison, the SPR distances (Fig. 7)

440 provide a broad indication of similarity, but lack the resolution required to make fine-scale
441 judgements.

442 *Geometric morphometrics*

443 The results of the geometric morphometric analysis (Fig. 9) compared to the result of the cladistic
444 analysis demonstrate that a short and broad distal expansion of the prepubis is an apomorphy of
445 Monofenestrata, shared by "*G. rhamphastinus*", *Diopecephalus* and *Darwinopterus*.
446 *Germanodactylus*, a more derived eupterodactyloid has a deeper distal expansion, whereas the
447 ctenochasmatooids and *Pterodactylus* have a more elongate/gracile diaphysis, but a plesiomorphic
448 shape to the distal expansion. The basal non-monofenestratans *Dorygnathus* and *Scaphognathus*
449 have a prominent bi-lobed distal expansion which distinguishes them from the monofenestratans.
450 The separation of non-monofenestratans from the monofenestratans supports the hypothesis that
451 the prepubis has a taxonomic utility, which has been overlooked in most previous analyses and
452 descriptions.

453 **Comparative anatomy**

454 *Pterodactylus and Diopecephalus*

455 The genera *Pterodactylus* and *Diopecephalus* are remarkably similar. However, the only cladistic
456 analyses to study both holotypes (Howse 1986; Vidovic and Martill 2014) find the two specimens in
457 distinct monophyletic clades or in a paraphyletic genus respectively. Furthermore, some – but not all
458 – morphometric bivariate plots (Vidovic and Martill 2014) demonstrate *Pterodactylus* to be more
459 closely associated with *Aerodactylus* than *Diopecephalus*, while *Aerodactylus* is distinguishable from
460 both species by its dentition, skull morphology and pteroid length.

461 Currently, there are just a few juvenile pterosaur specimens tentatively referred to *Diopecephalus*
462 (three including the holotype and a possible specimen figured by Arratia et al. [2015]) (Vidovic and
463 Martill 2014), rendering taxonomic work on a population impossible. However, using a typological
464 approach, the holotype of *Diopecephalus* does differ from *Pterodactylus* in that the cervical
465 vertebrae have a prominent spinous cranial hypapophysis (Howse 1986) and robust prominent
466 zygapophyses. Additionally, the manual unguals are less robust in *Diopecephalus* compared to
467 *Pterodactylus*, the diaphysis of the prepubis is more robust in *Diopecephalus* and the distal
468 expansion is broader than in *Pterodactylus* (Fig. 9). It was noted that *Diopecephalus* and
469 "*Pterodactylus elegans*" both lacked fusion of the atlas and axis and that the mid-cervical vertebrae
470 were approximately the same size, which was considered a plesiomorphic condition for the
471 Pterodactloidea by Howse (1986). However, due to their heterochrony, lack of fusion between

472 elements and those proportions of the mid-cervical vertebrae are common to juvenile
473 pterodactyloids (pers. obs.) (e.g. BSP 1967 I 276; BSP 1971 I 17; BSP 1936 I 50).

474 *Diopecephalus* and “*G. rhamphastinus*”

475 No conditions have been identified that *Diopecephalus* shares with *Pterodactylus* that it does not
476 also share with “*G. rhamphastinus*”. Despite their similarity, the relationship of *Diopecephalus* and
477 “*G. rhamphastinus*” has received little attention (Seeley 1871, 1901; Vidovic and Martill 2014). “*G.*
478 *rhamphastinus*” has been considered congeneric with *D. kochi* (Seeley 1871, 1901) and the type
479 species of *Germanodactylus* was originally referred to “*P. kochi*” (Plieninger 1901), but subsequent
480 to the separation of *D. kochi* and *Germanodactylus* spp. (Wiman 1925; Young 1964; Wellnhofer
481 1968, 1970) the species have been considered distinct without further discussion.

482 “*G. rhamphastinus*” and *Diopecephalus* share yet more conditions, including a prepubis with a
483 robust diaphysis and broad distal expansion, a more caudal extension of the dorsal process of the
484 premaxilla and less robust manual unguals than *Pterodactylus*. Other possible uniting characters are
485 tentative because they may be affected by ontogeny. For example, “*G. rhamphastinus*” has shorter
486 cervical vertebrae with more robust zygapophyses than *Pterodactylus*, similar to the condition in
487 *Diopecephalus* (Howse 1986).

488 “*G. rhamphastinus*” and *Pterodactylus*

489 “*G. rhamphastinus*” and *Pterodactylus* share conditions plesiomorphic to Monofenestrata and
490 Pterodactyloidea as discussed above. They differ in that “*G. rhamphastinus*” has a straighter slope to
491 the dorsal margin of the skull, pointed jaw tips, a steeper quadrate, fewer teeth in adult specimens,
492 a piriform orbit and a prepubis more similar to that of *Diopecephalus*. Notably, the *Pterodactylus*
493 specimen BMMS 7 was reconstructed using information available from *Aerodactylus* specimens
494 (Bennett 2013a), resulting in an overestimate of rostrum length and tooth number. It is likely that
495 the rostrum terminated shortly after the break in the rock and there were only 18 to 20 teeth in the
496 mature specimen’s jaws.

497 Although Bennett (1996) once suggested that the *Germanodactylus* spp. might represent more
498 mature specimens of *Pterodactylus* he subsequently changed his view (Bennett 2002 p.45). We
499 agree that some of the differences could be ontogenetically variable and perhaps vary between
500 sexes, so in 1996 it seemed possible that the two species could be at least congeneric. However,
501 more recent research has revealed more information on the ontogeny and phylogeny of
502 pterodactyloids (Jouve 2004; Bennett 2006, 2013a; Lü et al. 2009) and common opinion is that the
503 two are distinct genera.

504 *Germanodactylus cristatus* and “*Germanodactylus rhamphastinus*”
505 *Germanodactylus cristatus* differs from “*G. rhamphastinus*” and all other pterosaurs in that the
506 dentition is absent from the rostrum tip, but still present in the premaxilla. Wang et al. (2008) also
507 noted that the gestalt of the teeth differed between the two species. Also, the prepubis distal
508 expansion is cranioventrally long, making it approach a reuleaux triangle in outline. Additionally,
509 *Germanodactylus cristatus* has at least three fused dorsal vertebrae, which differs from the
510 condition in similarly sized “*G. rhamphastinus*”. These differences do not necessarily distinguish the
511 two species at the generic level. Indeed, Bennett (2006) considered the differences observed
512 between the two *Germanodactylus* species to diagnose the species within the genus. The two
513 species are seemingly united by a similar skull shape and an extreme caudal extension of the
514 premaxilla dorsal process, as well as some skeletal proportions (Bennett 2006 p.876). However,
515 these similarities are also observed in more basal and derived branches of Pterodactyloidea,
516 substantiating the claims that the genus is paraphyletic (Maisch et al. 2004; Vidovic and Martill 2014)
517 which is supported by the phylogeny presented here.

518 **Systematic palaeontology**

519 *DIOPECEPHALUS* Seeley, 1871

520 Fig. 1

521 Type species: *Diopecephalus kochi* (Wagner 1837)

522 Synonymy:

523 *1837 *Ornithocephalus kochii* Wagner 1837, p.164, pl.1.

524 1860 *Pterodactylus kochi* Wagler bei A. Wagner, 1837; Meyer 1860, p.35.

525 1871 *Diopecephalus kochi* (no author attributed); Seeley 1871, p.35.

526 1888 *Pterodactylus kochi* Wagner, 1837; Lydekker 1888, p.6.

527 1901 *Diopecephalus kochi* (no author attributed); Seeley 1901, p.168.

528 1882 *Pterodactylus kochi* (Wagler); Zittel 1882, p.18, pl.13, fig. 1.

529 1967 *Pterodactylus kochi* (Wagler); Kuhn 1967, p.16.

530 1968 *Pterodactylus kochi* (Wagner, 1837); Wellnhofer 1968, p.99.

531 1970 *Pterodactylus kochi* (Wagner, 1837); Wellnhofer 1970, p.22.

532 2004 *Pterodactylus antiquus* (Soemmerring, 1812); Jouve 2004, p.549.

533 Jouve considered "*P. kochi*" synonymous with *P. antiquus*.

534 2013 *Pterodactylus antiquus* (Soemmerring, 1812); Bennett 2013a, p.283.

535 2014 *Pterodactylus kochi* (Wagner, 1837); Vidovic and Martill 2014 p.1.

536 2014 *Diopecephalus kochi* (Wagner, 1837); Vidovic and Martill 2014 p.15.

537 Holotype: Part and counterpart, BSP AS XIX 3 and SMF R 404 (Fig. 1). A nearly complete skeleton on
538 a slab of limestone.

539 Referred material: An immature specimen represented by part and counterpart, NHM UK PV R 3949
540 and OUMNH JZ 1609. A privately owned specimen (Arratia et al. 2015: p.468, fig. 900) exhibited in
541 Museum Solnhofen.

542 Locality and horizon: Kelheim, Germany, Malm Zeta 3 (Wellnhofer 1970), or Malm Zeta 2
543 (Schweigert 2007), Lower Tithonian.

544 Genus and species diagnosis: (None of the following are autapomorphic, but are a unique
545 combination of characters) (1) A pterodactyloid pterosaur with an evenly sloping rostrum, leading
546 caudally into a rounded parietal region of the skull, with the dorsal process of the premaxilla
547 extending to the caudal region of a sub-rounded orbit. (2) Labiolingually compressed triangular teeth
548 are present from the jaw tip continuing caudally beneath the nasoantorbital fenestra. (3) The
549 longest cervical vertebra is 50% or less than the maximum skull depth, and no cervical vertebrae
550 exceed a length/depth quotient of 2.5. The cervical vertebrae have robust zygapophyses and an
551 enlarged spinous hypapophysis. (4) The prepubis flares abruptly to a broad distal expansion and its
552 maximum length is approximately equal to its maximum width.

553 Note: Combination 1 differs from *G. cristatus* and "*G. rhamphastinus*" in the parietal region of the
554 skull, and it differs from the condition in *Pterodactylus* in the caudal extent of the premaxilla.

555 Combination 2 differs from "*G. rhamphastinus*" and *Pterodactylus* in the tooth morphology, and it
556 also differs from *G. cristatus* in the distribution of that dentition. Combination 3 differs from
557 *Pterodactylus* but is similar to the conditions seen in *G. cristatus* and "*G. rhamphastinus*". Condition
558 4 is different to the morphologies observed in *G. cristatus* and *Pterodactylus*, but similar to that of
559 "*G. rhamphastinus*".

560 Remarks: Numerous examples of pterosaurs from the Solnhofen Limestone Formation have been
561 referred to "*P. kochi*" (e.g. Wellnhofer 1984; Tischlinger 1993; Frey and Martill 1998). In a recent
562 comparison of these examples and the holotype of *Diopecephalus*, they were excluded from the
563 taxon (Vidovic and Martill 2014). A perception may have arisen that *Diopecephalus kochi* occurs
564 frequently in the Tithonian limestones of Bavaria, Germany, but here it is regarded as a rare taxon.

565 Although technically the name "*Ornithocephalus kochii*" should be attributed to Wagner (1837),
566 many subsequent authors attribute it to Wagler in Wagner (1837) (Wellnhofer 1968). In fact,
567 although the name was devised by Wagler, and Wagner provided a reason to attribute it to Wagler
568 when he stated:

569 'Wagler wollte dem neu aufgefundenen Exemplare, das der Gegenstand vorliegender Abhandlung ist,
570 den Namen *Ornithocephalus Kochii* beilegen; ich behalte diese Benennung um so lieber bei, da mir
571 hiedurch Gelegenheit gegeben ist, dem würdigen Manne, der mit zuvorkommender Güte mir das
572 Original zur Publikation zukommen liess, ein geringes Denkmal meiner grossen Achtung und
573 Anerkennung zu setzen'

574 '[Wagler wanted the newly found specimens, which are the subject of this treatise, to be given the
575 name *Ornithocephalus kochii*. I keep this designation all the more gladly, because by doing so I am
576 given the opportunity to honor the worthy man, who courteously allowed the publication of the
577 original [material], a small monument of my great respect and recognition]'

578 ... there is no reason to credit the published name to Wagler (Wellnhofer 1968).

579 *ALTMUEHLOPTERUS* gen. nov.

580 LSID: urn:lsid:zoobank.org:act:81B99AC3-0475-4FB2-A879-DE3D6D540465

581 Derivation of name: "Altmuehl" refers to the Altmühl river that flows through Solnhofen (close to
582 Mörnsheim), Eichstätt and joins the river Danube at Kelheim. "Pterus" is a common suffix in
583 pterosaur names referring to the wing. This name is presented as an alternative to the
584 geographically significant name *Daitingopterus* (Maisch et al. 2004) which is a *nomen nudum*.

585 Type species: *Altmuehlopterus rhamphastinus* (Wagner 1851)

586 Fig. 2

587 Synonymy:

588 *1851 *Ornithocephalus ramphastinus* Wagner 1851, p.132, pl.1.

589 Note, here *ramphastinus* is spelled without the first letter 'h', named for its similarity to the
590 toucan *Ramphastos* (Bennett 2006).

591 1860 *Pterodactylus rhamphastinus* (Wagner, 1851); Meyer 1860, p.54.

592 Here Meyer makes the mistake of using an additional 'h' in the species name.

593 1861b *Pterodactylus rhamphastinus* no attribution; Wagner 1861b, p.531.

594 Wagner uses the emended spelling, seemingly accepting Meyer's *lapsus*.

595 1871 *Diopecephalus rhamphastinus* (Wagner, 1851); Seeley 1871, p.35.

596 1888 *Pterodactylus rhamphastinus* (Wagner); Lydekker 1888, p.8.

597 1927 *Pterodactylus rhamphatilus* (Wagner, 1851); Weigelt 1927, p.227, 28 Abb., Taf.37.

598 *Lapsus*. The 1989 English translation of Weigelt miscorrects this to *Germanodactylus*
599 *cristatus*.

600 1941 *Rhamphorhynchus kokeni* Plieninger, 1907; Edinger 1941, pp.671, 678.

601 1970 *Germanodactylus rhamphastinus* (Wagner, 1851); Wellnhofer 1970, p. 66.

602 1991 *Germanodactylus rhamphastinus* (Wagner, 1851); Wellnhofer 1991, p. 95.

603 1994 *Germanodactylus ramphastinus* (Wagner, 1851); Frickhinger 1994, p. 269.

604 Frickhinger returns to the original spelling of *ramphastinus*.

605 2004 *Daitingopterus rhamphastinus* no attribution; Maisch et al. 2004, p.631, table 1.

606 This name is a *nomen nudum* because the authors did not refer to a type specimen or state
607 that it was a new genus.

608 2006 *Germanodactylus rhamphastinus* (Wagner, 1851); Bennett 2006, p.877.

609 Bennett provides a detailed discussion of the synonymy.

610 2010 *Germanodactylus ramphastinus* (Wagner, 1851); Rodrigues et al. 2010, p.57.

611 These authors return to the original spelling of *ramphastinus*, but the emended spelling has
612 priority due to popular use.

613 Holotype: BSP AS I 745 a and counterpart BSP AS I 745 b (Fig. 2).

614 Referred material: MCZ 1886 adult specimen with dorsal soft tissue headcrest (Bennett 2002), JME
615 Moe 12 and counterpart BSP 1977 XIX 1 (Rodrigues et al. 2010).

616 Horizon and locality: Mörsheim Limestone Formation, Malm Zeta 3, Daiting, possibly Solnhofen
617 Formation, Solnhofen (see Bennett 2002).

618 Genus and species diagnosis: (None of the following are autapomorphic, but together comprise a
619 unique combination of characters) The dorsal process of the premaxilla supports a low, long crest,
620 which extends back level with the caudal margin of a tall orbit. The premaxilla forms an
621 approximately straight dorsal margin to the rostrum which terminates with a pointed rostrum tip.
622 Simple cone teeth (taller and thinner than in *Germanodactylus* and *Diopecephalus*) present at the
623 rostrum tip and below the nasoantorbital fenestra. There are ~16 widely spaced teeth in each jaw
624 that grade up in size and back down mesiodistally.

625 Remarks: The emended spelling of the name *rhamphastinus* (with the 'h') is used, as it has priority
626 through popular use (ICZN 33.3.1.). This seemed acceptable to Wagner (1861*b*).

627 The species is split from the genus *Germanodactylus* due to it only sharing conditions observed in
628 both more basal and more derived pterosaurs. The similarities observed between *Germanodactylus*
629 *cristatus* and *Altmuehlopterus rhamphastinus* are not considered to support their monophyly as a
630 single genus. This is supported by the results of a cladistic analysis and a geometric morphometric
631 analysis which indicate the condition of the prepubis in *Germanodactylus* is taxonomically
632 significant.

633

634 *GERMANODACTYLUS* (Young 1964)

635 Fig. 3

636 Type species: *Germanodactylus cristatus* (Wiman 1925)

637 Synonymy:

638 1901 *Pterodactylus kochi* Wagler; Plieninger 1901, p.65.

639 *1925 *Pterodactylus cristatus* Wiman 1925, p.17.

640 1964 *Germanodactylus kochi* (Wagler); Young 1964, p.251.

641 1967 *Diopecephalus kochi* (Wagler); Kuhn 1967, p.34.

642 1970 *Germanodactylus cristatus* (Wiman, 1925); Wellnhofer 1970, p.64.
643 1991 *Germanodactylus cristatus* (Wiman, 1925); Wellnhofer 1991, p.96.
644 2006 *Germanodactylus cristatus* (Wiman, 1925); Bennett 2006, p.873, figs 1-2.
645 2010 *Germanodactylus cristatus* (Wiman, 1925); Hone 2010, p.263, fig. 3.
646 Holotype: BSP 1892 IV 1: disarticulated, but near complete skeleton on a slab of Solnhofen
647 Limestone; Counterpart NMING F15005.
648 Referred material: JME SoS 4593, JME SoS 4006 (see Bennett 2006) and an undescribed specimen in
649 Karlsruhe (SMNK PAL 6529).
650 Horizon and locality: Solnhofen Limestone, Malm Zeta 2, Solnhofen, Germany.
651 Genus and species diagnosis: (Those characters marked with * are unique autapomorphies)
652 Pterodactyloid pterosaur with edentulous jaw tips but with short, triangular teeth present in the
653 remaining premaxilla. Prepubis with a reuleaux triangle shaped distal expansion* (Fig. 3 & 9).
654 Description: See (Wellnhofer 1970).
655 Remarks: The holotype of *Germanodactylus cristatus* can also be distinguished from other
656 pterosaurs by a unique suite of plesiomorphic and apomorphic characters including: approximately
657 50% of premaxillary rostrum ventral surface is comprised of the premaxilla; teeth are short, robust with
658 triangular outline in lateral view; tooth row extends beneath nasorostral fenestra; low, striated
659 bony crest present on adult individuals (this may be sexually dimorphic [see Bennett 1992; Lü et al.
660 2011; Wang et al. 2014] as a large specimen (SMNK PAL 6529) lacks such a crest); straight and
661 vertical orbit rostral margin; the wing-metacarpal is shorter than the ulna (Fig. 3); centra of dorsal
662 vertebrae 1–3 fused forming a small notarium.

663 **Discussion**

664 The dendrogram demonstrating the morphospace of pterosaur prepubes (Fig. 9) is in general
665 agreement with the phylogeny, suggesting that the prepubis morphology is of taxonomic value.
666 Conversely, the prepubis of *Pterodactylus* is in disagreement with the phylogeny, appearing more
667 similar to the ctenochasmatoid *Cycnorhamphus*, which is consistent with the results of other
668 cladistic analyses (Lü et al. 2009; Wang et al. 2009; Andres et al. 2014). However, in the geometric
669 morphometric analysis, the prepubis is only one anatomical unit expressing several characters across
670 10 specimens, compared to the 320 characters (including characters of the prepubis) and 99 OTUs of

671 the cladistic analysis. Furthermore, the dendrogram (Fig. 9) is constructed using hierarchical clusters,
672 akin to phenetics and is susceptible to the effects of homoplasy and reversibility (Camin and Sokal
673 1965). This methodology is far from a replacement for cladistic methods, but it does demonstrate
674 that the broad morphology of the prepubis can be used to understand the phylogenetic affinities of
675 pterosaurs (Fig. 9 and 10).

676 The cladistic analysis yields a strict consensus that places all four taxa with which this study is
677 concerned as basal pterodactyloid “transitional” taxa. *Pterodactylus* is the most basal branch of
678 these “transitional” taxa and the remaining three taxa are placed in Lophocratia (*Pterodaustro* +
679 *Quetzalcoatlus*). *Diopecephalus* is found in the monophyletic clade Euctenochasmata
680 (*Diopecephalus* + *Pterodaustro*), while *Altmuehlopterus* and *Germanodactylus* are found as basal
681 members of the Eupterodactyloidea (closer to *Pteranodon* than *Pterodaustro*). *Altmuehlopterus*
682 occupies a more basal position than *Germanodactylus*, which is to be expected given the number of
683 plesiomorphic conditions it possesses by comparison. Some derived conditions of *Germanodactylus*
684 (i.e. presence of a notarium) are shared with other dsungaripteroids, including ornithocheiroids and
685 azhdarchoids. However, the restricted dentition absent from the rostrum tip is seemingly an
686 autapomorphy of *Germanodactylus*, and convergent with dsungaripterines.

687 Many similarities observed between Solnhofen pterosaur specimens are a product of their early
688 ontogeny, lacking peramorphic conditions (Vidovic and Martill 2014) and the presence of their
689 shared plesiomorphic conditions. *Pterodactylus*, *Diopecephalus*, *Germanodactylus* and
690 *Altmuehlopterus* all share characters in common with the Painten pro-pterodactyloid (Tischlinger
691 and Frey 2013) and wukongopterids. These characters include an approximately triangular, laterally
692 compressed skull with a dentition extending under the nasoantorbital fenestra (Fig. 10). In some
693 cases the plesiomorphic low, long, striated bony headcrest is present (e.g. *Darwinopterus*,
694 *Germanodactylus* and *Altmuehlopterus*). The headcrest is a confounding structure, given that it is
695 sexually dimorphic and might not develop until sexual maturity is achieved, although juvenile
696 pterosaurs with small crests have been identified (Dalla Vecchia 2009; Vidovic and Martill 2014).
697 *Pterodactylus* and *Diopecephalus* are most similar to the Painten pro-pterodactyloid and this is
698 reflected in their position in the phylogeny (Fig. 4). Likewise, *Altmuehlopterus* has a remarkably
699 similar skull to *Darwinopterus* and *Cuspicephalus* (Martill and Etches 2012), but the skull of
700 *Altmuehlopterus* can be distinguished as pterodactyloid (Witton et al. 2015).

701 Despite being maintained as a *Pterodactylus* species for over a century, *Diopecephalus kochi* shares a
702 similar list of common characters with *Altmuehlopterus rhamphastinus*. Disregarding *Diopecephalus*,
703 the taxa *Pterodactylus*, *Altmuehlopterus*, and *Germanodactylus* are distinct and readily diagnosable.

704 Thus, *Diopecephalus* is the most problematic of these taxa. *Diopecephalus* could potentially
705 represent the juvenile condition of any of the other three genera discussed above, yet it is
706 phylogenetically placed as the most basal branch of the Euctenochasmatia (Unwin 2003) which
707 excludes these taxa. Vidovic and Martill (2014) demonstrated that *Pterodactylus* was more similar to
708 *Aerodactylus* than *Diopecephalus* in its skull, nasoantorbital fenestra and cervical vertebra
709 proportions. However, *Pterodactylus* is more similar to *Diopecephalus* in its dental distribution and
710 PCRW proportions to the skull. Likewise, *Altmuehlopterus* has the same plesiomorphic prepubis
711 condition and dental distribution as *Diopecephalus*, and both have a more caudal extension of the
712 premaxilla dorsal process than *Pterodactylus*. There are subtle differences between the
713 morphologies of *Altmuehlopterus* and *Diopecephalus* too. *Diopecephalus* has a more rounded
714 parietal region of the skull and teeth similar to those of *Germanodactylus* (labiolingually compressed
715 broad triangles) which differs from *Altmuehlopterus* (Wang et al. 2008). The mosaic of characters
716 that each taxon has in common demonstrates a complex evolutionary and ontogenetic relationship.
717 A privately owned specimen (Arratia et al. 2015) displayed in Museum Solnhofen demonstrates the
718 prepubis morphology and short cervical vertebrae with robust zygapophyses that distinguishes the
719 holotype of *Diopecephalus kochi* from *Pterodactylus* in a more mature individual. The specimen is
720 approximately the same size as the holotype of *Pterodactylus antiquus*, thus, the morphological
721 differences are unlikely to be ontogenetic in this specimen at least. Indeed, new examples may
722 provide further support for the taxon's validity. This situation raises the debate of species and taxon
723 concept, and how to deal with "transitional" taxa that demonstrate a mosaic of characters shared
724 amongst multiple taxa.

725 The genera, *Pterodactylus*, *Diopecephalus*, *Altmuehlopterus* and *Germanodactylus* have been
726 demonstrated to be valid monophyletic, monotypic taxa, despite their close similarities and mix of
727 characters. However, when examples of *D. kochi* are included in *Pterodactylus* and *A. rhamphastinus*
728 is included in *Germanodactylus* as has been asserted (Wellnhofer 1968, 1970; Jouve 2004; Bennett
729 2006, 2013a) (note, even taxonomic reviews that used empirical evidence [Jouve, 2004; Bennett
730 2013a] arguably suffered from the Texas sharpshooter fallacy and numerous explanations for the
731 same data could be given) these two genera are paraphyletic. That is to say, the common ancestor
732 of *P. antiquus* and *D. kochi* is also the common ancestor of higher taxa, including Ctenochasmatoidea
733 and Eupterodactyloidea. Likewise, the common ancestor of *A. rhamphastinus* and *G. cristatus* is
734 shared with the higher taxon Dsungaripteroidea. A monophyletic genus should comprise a natural
735 group of species that share a most recent common ancestor that is not shared with any other higher
736 taxa (Ebach and Williams 2010). Some proponents of Linnaean classification argue that it is a
737 theoretical impossibility to not have paraphyletic taxa (Brummitt 1997; Hörandl and Stuessy 2010).

738 At an impossibly fine resolution, one taxon does evolve from a subset of the population of another
739 taxon, rendering the progenitor taxon paraphyletic. However, to argue that one cannot artificially
740 scrutinize between one population and another because they are part of an evolutionary continuum
741 renders the use of both classification and cladification unsuitable. Indeed, if paraphyletic taxa were
742 permissible in a cladistic model and only monophyletic, polytypic taxa were regarded as valid, the
743 discovery of new fossil specimens would result in a continual reassessment of the taxonomy. This
744 problematic situation is observed in the higher clades of Pterosauria in the absence of a formalized
745 set of rules – for this purpose the PhyloCode has been proposed (Cantino and de Queiroz 2010).
746 Therefore, to provide phyletic and nomenclatural (Queiroz 2006) stability to the four species with
747 which this study is concerned they must occupy four distinct genera based on positive evidence of
748 monophyly, not an assertion or negative evidence – recency of the common ancestor, not similarity.

749 Despite a taxonomic resolution the case remains that the four taxa with which this study is
750 concerned are “transitional” monotypic taxa, which has proven especially problematic in the case of
751 *Pterodactylus*, *Diopecephalus*, and *Altmuehlopterus*. Taxon concepts are based on a “snapshot” of
752 organisms during a point in their evolution, either in the present day or in the fossil record. Thus,
753 there is a general misconception that taxa are biologically distinct entities. We are fortunate that the
754 Franconia laminated limestones provide a series of successive “snapshots” through a geologically
755 short period (Fig. 10). This situation provides an unparalleled understanding of pterosaur evolution
756 and ecological niche partitioning, but it also exposes the blurred lines of the taxon concept.

757 In the Franconia laminated limestones there is a succession of monofenestratan pterosaurs present,
758 from the Painten pro-pterodactyloid (Tischlinger and Frey 2013) through to *Germanodactylus*.
759 Pterosaurs from the Hybonotum Zone are numerous, by contrast with the Beckeri Zone. Clearly, by
760 the start of the Tithonian, most of the non-dsungaripteroid pterosaur diversity had appeared.
761 Further exploration of the laminated limestones in the Beckeri Zone could provide much more
762 evidence for early pterodactyloid evolution and development.

763 **Acknowledgements**

764 Oliver Rauhut, Marcus Moser (Munich), Lorna Steel (London), Eliza Howlett (Oxford), Loic Costeur,
765 Christian Meyer (Basel) and Rainer Brocke (Frankfurt) are thanked for access to specimens in their
766 care. Lorna Steel and Eliza Howlett are especially thanked for their help tracing the history of two
767 specimens. Bob Loveridge and John Vidovic are thanked for providing photographs. DMM would like
768 to thank Helmut Tischlinger for access to his personal library. Finally, we would like to thank the Willi
769 Hennig Society and contributors to R for making their software and packages freely available.

770

771

772

773 **References**

- 774 ADAMS, D. C. & OTÁROLA-CASTILLO, E. 2013. Geomorph: an R package for the collection and
775 analysis of geometric morphometric shape data. *Methods in Ecology and Evolution*, **4**, 393–
776 399.
- 777 ANDRES, B. & JI, Q. 2008. A new pterosaur from the Liaoning province of China, the phylogeny of the
778 Pterodactyloidea, and convergence in their cervical vertebrae. *Palaeontology*, **51**, 453–469.
- 779 ANDRES, B., CLARK, J. & XU, X. 2014. The earliest pterodactyloid and the origin of the group. *Current*
780 *Biology*, **24**, 1011–1016.
- 781 ARCHIBALD, J. D. 1994. Metataxon concepts and assessing possible ancestry using phylogenetic
782 systematics. *Systematic Biology*, **43**, 27–40.
- 783 ARRATIA, G., SCHULTZE, H.-P., TISCHLINGER, H. & VIOHL, G. 2015. *Solnhofen - Ein Fenster in die*
784 *Jurazeit 1+2*. Pfeil, F.
- 785 ARTHABER, G. 1919. Studien über Flugsaurier auf grund der bearbeitung des Wiener exemplares von
786 *Dorygnathus Banthensis* Theod. sp. *Denkschrift der Akademie der Wissenschaften Wien,*
787 *Mathematisch-Naturwissenschaftliche Klasse*, **97**, 391-464.
- 788 BELL, M. A. & LLOYD, G. T. 2014. *Strap: Stratigraphic Tree Analysis for Palaeontology*. R package
789 version 1.4. <https://CRAN.R-project.org/package=strap>.
- 790 BENNETT, S. C. 1992. Sexual dimorphism of *Pteranodon* and other pterosaurs, with comments on
791 cranial crests. *Journal of Vertebrate Paleontology*, **12**, 422–434.
- 792 BENNETT, S. C. 1994. *Taxonomy and systematics of the Late Cretaceous pterosaur Pteranodon*
793 *(Pterosauria, Pterodactyloida)*. Occasional Papers of the Natural History Museum, University
794 of Kansas, **169**, 1–70.
- 795 BENNETT, S. C. 1996. Year-classes of pterosaurs from the Solnhofen Limestone of Germany:
796 taxonomic and systematic implications. *Journal of Vertebrate Paleontology*, **16**, 432–444.
- 797 BENNETT, S. C. 2002. Soft tissue preservation of the cranial crest of the pterosaur *Germanodactylus*
798 from Solnhofen. *Journal of Vertebrate Paleontology*, **22**, 43–48.
- 799 BENNETT, S. C. 2006. Juvenile specimens of the pterosaur *Germanodactylus cristatus*, with a review
800 of the genus. *Journal of Vertebrate Paleontology*, **26**, 872–878.
- 801 BENNETT, S. C. 2013a. New information on body size and cranial display structures of *Pterodactylus*
802 *antiquus*, with a revision of the genus. *Paläontologische Zeitschrift*, **87**, 269–289.
- 803 BENNETT, S. C. 2013b. The phylogenetic position of the Pterosauria within the Archosauromorpha
804 re-examined. *Historical Biology*, **25**, 545–563.
- 805 BONAPARTE, J. F. 1970. *Pterodaustro guinazui* gen. et sp. nov. Pterosaurio de la Formacion Lagarcito,
806 Provincia de San Luis, Argentina y su significado en la geologia regional (Pterodactylidae).
807 *Acta Geologica Lilloana*, **10**, 209–225.
- 808 BRAZEAU, M. D. 2011. Problematic character coding methods in morphology and their effects.
809 *Biological Journal of the Linnean Society*, **104**, 489–498.
- 810 BRUMMITT, R. K. 1997. Taxonomy versus cladonomy, a fundamental controversy in biological
811 systematics. *Taxon*, **46**, 723–734.
- 812 CAMIN, J. H. & SOKAL, R. R. 1965. A method for deducing branching sequences in phylogeny.
813 *Evolution*, **19**, 311–326.
- 814 CANTINO, P. D. & DE QUEIROZ, K. 2010. International code of phylogenetic nomenclature. *Version*
815 *4c*. [Online.] Available from: [http://www.ohio.edu/phylocode/\(accessed 30 May 2013\)](http://www.ohio.edu/phylocode/(accessed 30 May 2013)).
- 816 CARPENTER, K., UNWIN, D., CLOWARD, K., MILES, C. & MILES, C. 2003. A new scaphognathine
817 pterosaur from the Upper Jurassic Morrison Formation of Wyoming, USA. *Geological Society,*
818 *London, Special Publications*, **217**, 45–54.
- 819 COLLESS, D. H. 1980. Congruence between morphometric and allozyme data for *Menidia* species: A
820 reappraisal. *Systematic Zoology*, **29**, 288–299.
- 821 CUVIER, G. 1809. Mémoire sur le squelette fossile d'un reptile volant desenvirons d Aichstedt, que
822 les naturalistes ont pris pour un oiseau, et dont nous formons un genre de sauriens, sous le
823 nom de Ptero-Dactyle. *Annales du Muséum d'Histoire Naturelle*, **13**, 424–437.

- 824 DALLA VECCHIA, F. M. 2009. The first Italian specimen of *Austriadactylus cristatus* (Diapsida,
825 Pterosauria) from the Norian (Upper Triassic) of the Carnic Prealps. *Rivista Italiana di*
826 *Paleontologia e Stratigrafia [Research in Paleontology and Stratigraphy]*, **115**, 291–304.
- 827 DALLA VECCHIA, F. M., WILD, R., HOPF, H. & REITNER, J. 2002. A crested rhamphorhynchoid
828 pterosaur from the Late Triassic of Austria. *Journal of Vertebrate Paleontology*, **22**, 196–199.
- 829 EBACH, M. C. & WILLIAMS, D. M. 2010. Aphyly: a systematic designation for a taxonomic problem.
830 *Evolutionary biology*, **37**, 123–127.
- 831 EDINGER, T. 1941. The brain of *Pterodactylus*. *American Journal of Science*, **239**, 665–682.
- 832 FABRE, J. 1976. Un nouveau Pterodactylidae sur le gisement “Portlandian” de Canjurs (Var):
833 *Gallodactylus canjuersensis* nov. gen., nov. sp. *Comptes Rendus de l’Academie des Science,*
834 *Paris*, **279**, 2011–2014.
- 835 FIORINI, N., LEFORT, V., CHEVENET, F., BERRY, V. & CHIFOLLEAU, A.-M. A. 2014. CompPhy: a web-
836 based collaborative platform for comparing phylogenies. *BMC evolutionary biology*, **14**, 253.
- 837 FREY, E. & MARTILL, D. M. 1998. Soft tissue preservation in a specimen of *Pterodactylus kochi*
838 (WAGNER) from the Upper Jurassic of Germany. *Neues Jahrbuch für Geologie und*
839 *Palaontologie-Abhandlungen*, **210**, 421–441.
- 840 FREY, E., MEYER, C. A. & TISCHLINGER, H. 2011. The oldest azhdarchoid pterosaur from the Late
841 Jurassic Solnhofen Limestone (Early Tithonian) of Southern Germany. *Swiss Journal of*
842 *Geosciences*, **104**, 35–55.
- 843 FRICKHINGER, K. A. 1994. *Die Fossilien von Solnhofen: Dokumentation der aus den Plattenkalken*
844 *bekanntesten Tiere und Pflanzen*. Vol. 1. Goldschneck-Verlag.
- 845 GALILI, T. 2015. Dendextend: an R package for visualizing, adjusting and comparing trees of
846 hierarchical clustering. *Bioinformatics*: btv428.
- 847 GOLOBOFF, P. A. 2008. Calculating SPR distances between trees. *Cladistics*, **24**, 591–597.
- 848 GOLOBOFF, P. A. 2014. Extended implied weighting. *Cladistics*, **30**, 260–272.
- 849 GOLOBOFF, P. A., FARRIS, J. S. & NIXON, K. C. 2008a. TNT, a free program for phylogenetic analysis.
850 *Cladistics*, **24**, 774–786.
- 851 GOLOBOFF, P. A., CARPENTER, J. M., ARIAS, J. S. & ESQUIVEL, D. R. M. 2008b. Weighting against
852 homoplasy improves phylogenetic analysis of morphological data sets. *Cladistics*, **24**, 758–
853 773.
- 854 HONE, D. W. 2010. A short note on modifications to nineteenth century pterosaur specimens held in
855 the National Museum of Ireland–Natural History, Dublin. *Geological Curator*, **9**, 261–265.
- 856 HÖRANDL, E. & STUESSY, T. F. 2010. Paraphyletic groups as natural units of biological classification.
857 *Taxon*, **59**, 1641–1653.
- 858 HOWSE, S. C. B. 1986. On the cervical vertebrae of the Pterodactyloidea (Reptilia: Archosauria).
859 *Zoological Journal of the Linnean Society*, **88**, 307–328.
- 860 HUENE, F. VON. 1951. Zwei ausgezeichnet erhaltene Exemplare von *Pterodactylus* im Natur-
861 Museum Senckenberg. *Senckenbergiana*, **32**, 1–7.
- 862 JOUVE, S. 2004. Description of the skull of a *Ctenochasma* (Pterosauria) from the latest Jurassic of
863 eastern France, with a taxonomic revision of European Tithonian Pterodactyloidea. *Journal*
864 *of Vertebrate Paleontology*, **24**, 542–554.
- 865 KELLNER, A. W. A. 2003. Pterosaur phylogeny and comments on the evolutionary history of the
866 group. *Geological Society, London, Special Publications*, **217**, 105–137.
- 867 KUHN, O. 1967. *Die fossile Wirbeltierklasse Pterosauria*. Oeben, Krailing bei München, 52 pp.
- 868 LAWSON, D. A. 1975. Pterosaur from the latest Cretaceous of West Texas: discovery of the largest
869 flying creature. *Science*, **187**, 947–948.
- 870 LÜ, J. 2009. A new non-pterodactyloid pterosaur from Qinglong County, Hebei Province of China.
871 *Acta Geologica Sinica - English Edition*, **83**, 189–199.
- 872 LÜ, J. & JI, Q. 2006. Preliminary results of a phylogenetic analysis of the pterosaurs from western
873 Liaoning and surrounding areas. *Journal of Paleontological Society of Korea*, **22**, 239–261.

- 874 LÜ, J., JI, S., YUAN, C. & JI, Q. 2006. [Chapter 4: Phylogenetic analysis of the relationships of Chinese
875 pterosaurs]. In: [Pterosaurs from China], Geological Publishing House, Beijing.
- 876 LÜ, J., UNWIN, D. M., JIN, X., LIU, Y. & JI, Q. 2009. Evidence for modular evolution in a long-tailed
877 pterosaur with a pterodactyloid skull. *Proceedings of the Royal Society of London B:*
878 *Biological Sciences*: rspb20091603.
- 879 LÜ, J., UNWIN, D. M., DEEMING, D. C., JIN, X., LIU, Y. & JI, Q. 2011. An egg-adult association, gender,
880 and reproduction in pterosaurs. *Science*, **331**, 321–324.
- 881 LYDEKKER, R. 1888. *Catalogue of the fossil reptilia and amphibia in the British Museum (Natural*
882 *History)*. Vol. 1. order of the Trustees, 309 pp.
- 883 MAISCH, M. W., MATZKE, A. T. & SUN, G. 2004. A new dsungaripteroid pterosaur from the Lower
884 Cretaceous of the southern Junggar Basin, north-west China. *Cretaceous Research*, **25**, 625–
885 634.
- 886 MARSH, O. C. 1876a. Principal characters of American pterodactyls. *American Journal of Science*, **72**,
887 479–480.
- 888 MARSH, O. C. 1876b. Notice of a new sub-order of Pterosauria. *American Journal of Science*, **11**,
889 507–509.
- 890 MARTILL, D. M. & ETCHES, S. 2012. A new monofenestratan pterosaur from the Kimmeridge Clay
891 Formation (Kimmeridgian, Upper Jurassic) of Dorset, England. *Acta Palaeontologica*
892 *Polonica*, **58**, 285–294.
- 893 MARTILL, D. M., VIDOVIC, S. U., HOWELLS, C. & NUDDS, J. R. 2016. The Oldest Jurassic Dinosaur: A
894 Basal Neotheropod from the Hettangian of Great Britain. *PLoS ONE*, **11**, e0145713.
- 895 MEYER, H. 1834. *Gnathosaurus subulatus*, ein Saurus aus dem lithographischen Schiefer von
896 Solnhofen. *Museum Senckenbergianum*, **1**, 5–7.
- 897 MEYER, H. 1852. *Ctenochasma römeri*. *Palaeontographica*, **2**, 82–84.
- 898 MEYER, H. 1854. *Pterodactylus longicollum* n. sp. In: *Solenhofener Schiefer. Neues Jahrbuch für*
899 *Mineralogie, Geognosie, Geologie und Petrefakten-Kunde. Briefwechsel Mittheilungen an*
900 *Professor Bronn*, 51–56.
- 901 MEYER, H. 1856. *Pt. micronyx* n. sp. Neues Jahrbuch für Mineralogie, Geognosie, Geologie und
902 Petrefakten-Kunde. Briefwechsel Mittheilungen an Professor Bronn, 826–827.
- 903 MEYER, H. 1860. Zur Fauna der Vorwelt: Reptilien aus dem lithographischen Schiefer des Jura in
904 Deutschland und Frankreich. Briefliche Mittheilungen an Professor Bronn, 1–84.
- 905 MEYER, R. K. 1977. Stratigraphie und Fazies des Frankendolomits und der Massenkalk (Malm). In:
906 *Südliche Frankenalb*. Erlanger geologische Abhandlungen, **104**.
- 907 MONGIARDINO KOCH, N., SOTO, I. M. & RAMÍREZ, M. J. 2015. Overcoming problems with the use of
908 ratios as continuous characters for phylogenetic analyses. *Zoologica Scripta*, **44**, 463–474.
- 909 NESBITT, S. J., SMITH, N. D., IRMIS, R. B., TURNER, A. H., DOWNS, A. & NORELL, M. A. 2009. A
910 complete skeleton of a Late Triassic saurischian and the early evolution of dinosaurs.
911 *Science*, **326**, 1530–1533.
- 912 NESOV, L. A. 1984. [Pterosaurs and birds from the Late Cretaceous of Middle Asia].
913 *Paleontologicheskii Zhurnal*, **1984**, 45–57.
- 914 OWEN, R. 1859. On a new genus (*Dimorphodon*) of pterodactyle, with remarks on the geological
915 distribution of flying reptiles. *Report for the British Association for the Advancement of*
916 *Science*, **28**, 97–103.
- 917 PEREYRA, V. & MOUND, L. A. 2009. Phylogenetic relationships within the genus *Cranothrips*
918 (Thysanoptera, Melanthripidae) with consideration of host associations and disjunct
919 distributions within the family. *Systematic Entomology*, **34**, 151–161.
- 920 PLIENINGER, F. 1901. Beiträge zur Kenntnis der Flugsaurier. *Palaeontographica*, **48**, 65–90.
- 921 PLIENINGER, F. 1907. Die Pterosaurier der Juraformation Swabens. *Palaeontographica*, **53**, 209–313.
- 922 QUEIROZ, K. DE. 2006. The PhyloCode and the Distinction between Taxonomy and Nomenclature.
923 *Systematic Biology*, **55**, 160–162.

- 924 QUENSTEDT, F. A. 1855. Über *Pterodactylus suevicus* im lithographischen Schiefer Württembergs. 1–
925 52. Universität Tübingen, Tübingen.
- 926 REVELL, L. J. 2012. Phytools: An R package for phylogenetic comparative biology (and other things).
927 *Methods in Ecology and Evolution*, **3**, 217–223.
- 928 ROBINSON, D. F. & FOULDS, L. R. 1981. Comparison of phylogenetic trees. *Mathematical Biosciences*,
929 **53**, 131–147.
- 930 RODRIGUES, T., KELLNER, A. W. A. & RAUHUT, O. 2010. A new specimen of the
931 archaeoptero-dactyloid *Germanodactylus ramphastinus*. *Acta Geoscientica Sinica* **31** (Supp.
932 1), 57–58.
- 933 ROHLF, F. J. 2010. *TpsDig, digitize landmarks and outlines, ver. 2.16*.
- 934 SCHWEIGERT, G. 2007. Ammonite biostratigraphy as a tool for dating Upper Jurassic lithographic
935 limestones from South Germany – first results and open questions. *Neues Jahrbuch für*
936 *Geologie und Paläontologie - Abhandlungen*, **245**, 117–125.
- 937 SEELEY, H. G. 1870. *The Ornithosauria: an elementary study of the bones of pterodactyles*. Deighton,
938 Bell, and Co., Cambridge, 137 pp.
- 939 SEELEY, H. G. 1871. III.—Additional evidence of the structure of the head in Ornithosaurs from the
940 Cambridge Upper Greensand; being a supplement to 'The Ornithosauria'. *Journal of Natural*
941 *History*, **7**, 20–36.
- 942 SEELEY, H. G. 1901. *Dragons of the Air - An Account of Extinct Flying Reptiles*. Methuen and Co, 239
943 pp.
- 944 SÖMMERRING, S. 1812. Über einen *Ornithocephalus*. *Denkschrift der Königlichen Akademie*
945 *Wissenschaften, München*, **3**, 89–120.
- 946 SULLIVAN, C., WANG, Y., HONE, D. W. E., WANG, Y., XU, X. & ZHANG, F. 2014. The Vertebrates of the
947 Jurassic Daohugou Biota of Northeastern China. *Journal of Vertebrate Paleontology*, **34**, 243–80.
- 948 TISCHLINGER, H. 1993. Überlegungen zur Lebensweise der Pterosaurier anhand eines verheilten
949 Oberschenkelbruches bei *Pterodactylus kochi* (Wagner). *Archaeopteryx*, **11**, 63–71.
- 950 TISCHLINGER, H. & FREY, E. 2013. Ein neuer Pterosaurier mit Mosaikmerkmalen basaler und
951 pterodactyloider Pterosauria aus dem Ober-Kimmeridgium von Painten (Oberpfalz,
952 Deutschland). *Archaeopteryx*, **31**, 1–13.
- 953 UNWIN, D. M. 2003. On the phylogeny and evolutionary history of pterosaurs. *Geological Society*,
954 *London, Special Publications*, **217**, 139–190.
- 955 VIDOVIC, S. U. & MARTILL, D. M. 2014. *Pterodactylus scolopaciceps* Meyer, 1860 (Pterosauria,
956 Pterodactyloidea) from the Upper Jurassic of Bavaria, Germany: the problem of cryptic
957 pterosaur taxa in early ontogeny. *PLoS ONE*, **9**, e110646.
- 958 WAGNER, A. 1837. Beschreibung eines neu entdeckten *Ornithocephalus*: nebst allgemeinen
959 Bemerkungen über die Organisation dieser Gattung. *Abhandlungen der Bayerische Akademie*
960 *der Wissenschaften Mathematisch-Wissenschaftlichen Klasse*, **2**, 165–198.
- 961 WAGNER, A. 1851. Beschreibung einer neuen Art von *Ornithocephalus* etc. *Abhandlungen*
962 *Bayerischen Akademie für Wissenschaften Mathematisch-Physikalische Klasse*, (1850), 127–
963 192.
- 964 WAGNER, A. 1858. Neue Beiträge zur Kenntnis der urweltlichen Fauna des lithographischen
965 Schiefers. *Abteilung, Saurier. Abhandlungen der Bayerische Akademie der Wissenschaften*
966 *Mathematisch-Wissenschaftlichen Klasse*, **8**, 417–528.
- 967 WAGNER, A. 1860. Bemerkungen über die Arten von Fische und Saurier, welche im untern wie im
968 oberen Lias zugleich vorkommen sollen. *Sitzungsberichte der Konigliche Bayerischen*
969 *Akademie der Wissenschaften Mathematisch-physik Klasse*, (1860), 36–52.
- 970 WAGNER, A. 1861a. Charakteristik einer neuen Flugeidechie, *Pterodactylus elegans*. *Sitzungsberichte*
971 *der königlich bayerischen Akademie der Wissenschaften Mathematisch-physik Klasse*, (1861),
972 363 p.

- 973 WAGNER, A. 1861b. Übersicht über die fossilen Reptilen des lithographischen Schiefers in Bayern
974 nach ihren Gattungen und Arten. *Sitzungsberichte der königlich bayerischen Akademie der*
975 *Wissenschaften Mathematisch-physik Klasse*, (1861), 467–535.
- 976 WANG, X., CAMPOS, D. D. A., ZHOU, Z. & KELLNER, A. W. 2008. A primitive istiodactylid pterosaur
977 (Pterodactyloidea) from the Jiufotang Formation (Early Cretaceous), northeast China.
978 *Zootaxa*, (1813), 1–18.
- 979 WANG, X., KELLNER, A. W. A., JIANG, S. & MENG, X. 2009. An unusual long-tailed pterosaur with
980 elongated neck from western Liaoning of China. *Anais da Academia Brasileira de Ciências*,
981 **81**, 793–812.
- 982 WANG, X., KELLNER, A. W. A., JIANG, S., WANG, Q., MA, Y., PAIDOUOLA, Y., CHENG, X., RODRIGUES, T.,
983 MENG, X., ZHANG, J., LI, N. & ZHOU, Z. 2014. Sexually Dimorphic Tridimensionally Preserved
984 Pterosaurs and Their Eggs from China. *Current Biology*, **24**, 1323–1330.
- 985 WEIGELT, J. 1927. *Rezente Wirbeltierleichen und ihre paläobiologische Bedeutung*. Leipzig, verlag
986 Max Weg, 227 pp.
- 987 WELLNHOFER, P. 1968. Über *Pterodactylus kochi* (Wagner 1837). *Neues Jahrbuch für Geologie und*
988 *Paläontologie, Abhandlungen*, **132**, 97–126.
- 989 WELLNHOFER, P. 1970. Die Pterodactyloidea (Pterosauria) der Oberjura-Plattenkalke
990 Suddeutschlands. *Bayerische Akademie der Wissenschaften, Mathematisch-*
991 *Wissenschaftlichen Klasse, Abhandlungen*, **141**, 1–133.
- 992 WELLNHOFER, P. 1984. Die Flughaut von *Pterodactylus* (Reptilia, Pterosauria) am Beispiel des Wiener
993 Exemplares von *Pterodactylus kochi* (Wagner). *Annalen des Naturhistorischen Museums in*
994 *Wien. Serie A für Mineralogie und Petrographie, Geologie und Paläontologie, Anthropologie*
995 *und Prähistorie*, **88**, 149–162.
- 996 WELLNHOFER, P. 1991. *The illustrated encyclopedia of pterosaurs*. Crescent Books.
- 997 WILD, R. 1983. A new pterosaur (Reptilia, Pterosauria) from the Upper Triassic (Norian) of Friuli,
998 Italy. *Gortania - Atti del Museo Friulano di Storia Naturale*, **5**, 45–62.
- 999 WILLS, M. A. 1999. Congruence between phylogeny and stratigraphy: randomization tests and the
1000 Gap Excess Ratio. *Systematic Biology*, **48**, 559–580.
- 1001 WIMAN, C. 1925. Über *Pterodactylus Westmani* und andere Flugsaurier. *Bulletin of the Geological*
1002 *Institution of the University of Uppsala*, **20**, 1–38.
- 1003 WITTON, M. P., O'SULLIVAN, M. AND MARTILL, D. M. 2015. The relationships of *Cuspicephalus scarfi*
1004 Martill and Etches, 2013 and *Normannognathus wellnhoferi* Buffetaut et al., 1998 to other
1005 monofenestratan pterosaurs. *Contributions to Zoology*, **84**, 115–127.
- 1006 YOUNG, C. C. 1964. On a new pterosaurian from Sinkiang, China. *Vertebrata Palasiatica*, **8**, 221–255.
- 1007 YOUNG, C. C. 1973. Reports of Paleontological Expedition to Sinkiang (II). Pterosaurian Fauna from
1008 Wuerho, Sinkiang. *Mem. Inst. Vert. Palaeont. Paleoanthr. Acad. Sin.* **11**, 18–35.
- 1009 ZITTEL, K. A. 1882. Über Flugsaurier aus dem lithographischen Schiefer Bayerns. *Palaeontographica*,
1010 (1846-1933), 47–80.
- 1011

Table 1. *monofenestratans from Franconia laminated limestone localities*

Malm Zeta 1	Malm Zeta 2	Malm Zeta 3
Upper Kimmeridgian	Lower Tithonian	Lower Tithonian
<i>Cycnorhamphus suevicus</i> (Quenstedt 1855) (holotype)	<i>Pterodactylus antiquus</i> (Sömmerring 1812) (holotype)	<i>Diopcephalus kochi</i> (Wagner 1837)?
<i>Ardeadactylus longicollum</i> (Meyer 1854) (neotype)	<i>Gnathosaurus subulatus</i> Meyer 1834	" <i>Germanodactylus</i> <i>rhamphastinus</i> " (Wagner 1851)
Painten pro-pterodactyloid (<i>sensu</i> Tischlinger and Frey 2013)	<i>Aurorazhdarcho micronyx</i> (Meyer 1856)	<i>Pterodactylus antiquus</i> (Sömmerring 1812) (Bennett 2013a) (BMMS 7)
<i>Pterodactylus c.f. antiquus</i> (SMF R 4072)	(Meyer 1860)	
	<i>Ctenochasma elegans</i> (Wagner 1861a)	
	<i>Germanodactylus cristatus</i> (Wiman 1925)	
	<i>Ardeadactylus longicollum</i> (Meyer 1854) (lost holotype)*	

1013 *Note that the lost holotype of "*Pterodactylus longicollum*" may represent another

1014 aurorazhdarchian

1015

1016

1017 **Fig. 1.** *Diopcephalus kochi* - photographs and interpretative drawings of the slabs (a) SMF R 404 and
 1018 (b) BSP AS XIX 3. Abbreviations: a, articular; co, coracoid; cv, cervical vertebra; d, dentary; dv, dorsal
 1019 vertebra; f, femur; fr, frontal; h, humerus; ip, ischiopubic plate; j, jugal; l, lacrimal; mt, metatarsal;
 1020 mu, manual unguals; mx, maxilla; n, nasal; naof, nasoantorbital fenestra; o, orbit; p, parietal; pa,
 1021 preacetabular process; pd, pedal digit; pd5, pedal digit 5; pmx, premaxilla; po, post-orbital; poa,
 1022 postacetabular process; pp, prepubis; pt, pteroid; pu, pedal unguals; q, quadrate; qj, quadratojugal;
 1023 ra, radius; ri, ribs; sc, scapula; sq, squamosal; sv, sacral vertebra; ti, tibia; u, ulna; wmc, wing
 1024 metacarpal; wph1-4, wing phalanx 1-4.

1025

1026 **Fig. 2.** “*Germanodactylus rhamphastinus*” - photographs and interpretative drawings of the slabs (a)
1027 BSP AS I 745 b and (b) BSP AS I 745 a. Abbreviations: pc, premaxillary crest; st, sternum.

1028

1029 **Fig. 3.** *Germanodactylus cristatus* - (a) a photograph of most of the skeleton on the slab and (b) a line
1030 drawing of the skull of the holotype BSP 1892 IV 1.

1031

1032 **Fig. 4.** Strict consensus cladogram of two trees found using a “new technology” search in TNT,
1033 analysing 104 taxa and 320 characters. The tree is plotted stratigraphically using Phytools and Strap,
1034 and the GER (Wills, 1999) is given on the top right. The four taxa with which this study is concerned
1035 are given in bold.

1036

1037 **Fig. 5.** Results of the CRI between the taxon reduced trees of Maisch et al. (2004), Lü et al. (2010),
1038 Wang et al. (2009), Andres et al. (2014) and the tree presented here. CRI values are reported on the
1039 upper right. Analyses with polytomies in their source trees are indicated by an asterisk. On the lower
1040 left there are pie charts indicating tree similarity (corresponding to diagonally symmetrical values);
1041 dark slices represent agreement; lighter slices represent disagreement.

1042 **Fig. 6.** Robinson-Foulds (R-F) distances between the taxon reduced trees of Maisch et al. (2004), Lü
1043 et al. (2010), Wang et al. (2009), Andres et al. (2014) and the tree presented here. On the upper right
1044 the R-F distances from TNT are reported first, the colon is followed by the “proper” R-F distance
1045 calculated in CompPhy. On the lower left there are pie charts indicating tree similarity
1046 (corresponding to diagonally symmetrical values); dark slices represent agreement; lighter slices
1047 represent disagreement.

1048 **Fig. 7.** SPR distances (Goloboff 2008) between the taxon reduced trees of Maisch et al. (2004), Lü et
1049 al. (2010), Wang et al. (2009), Andres et al. (2014) and the tree presented here. SPR distances are
1050 reported on the upper right. On the lower left are pie charts indicating the similarity (corresponding
1051 to diagonally symmetrical values); dark slices represent agreement; lighter slices represent
1052 disagreement.

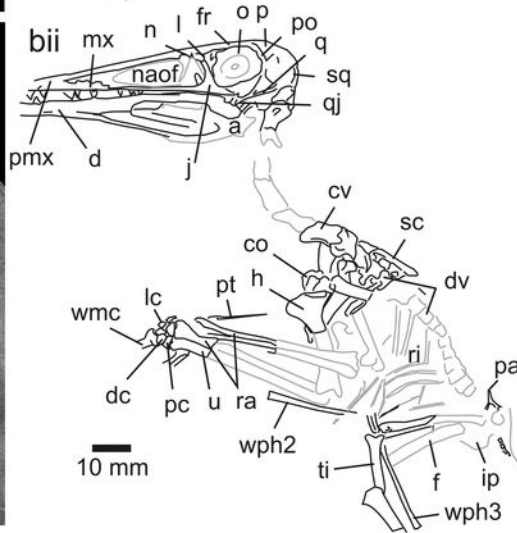
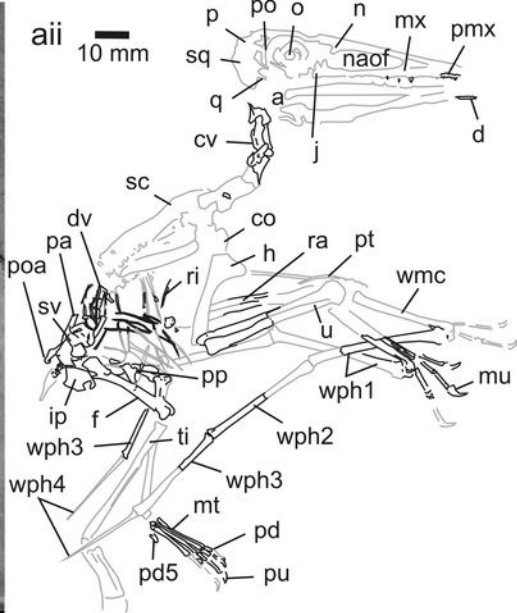
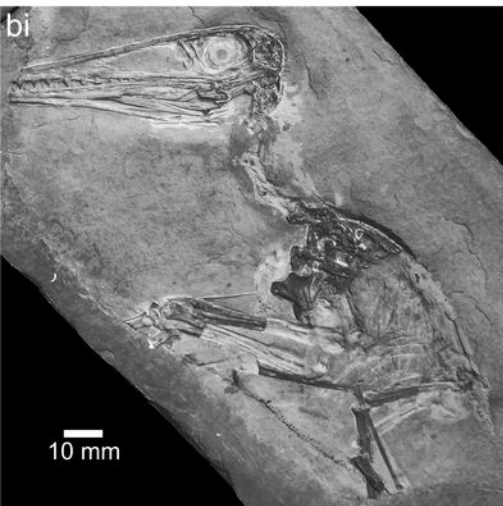
1053 **Fig. 8.** Tanglegrams of three cladograms that demonstrate a paraphyletic *Germanodactylus*, each
1054 recovered in a distinct cladistic analysis. (a) The cladogram of Maisch et al. (2004) and the cladogram
1055 presented here. It is possible that Maisch et al. (2004) coded a specimen of *Aerodactylus* previously

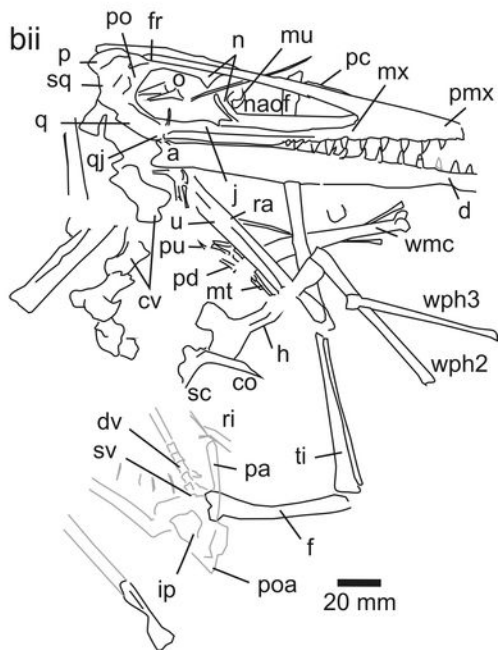
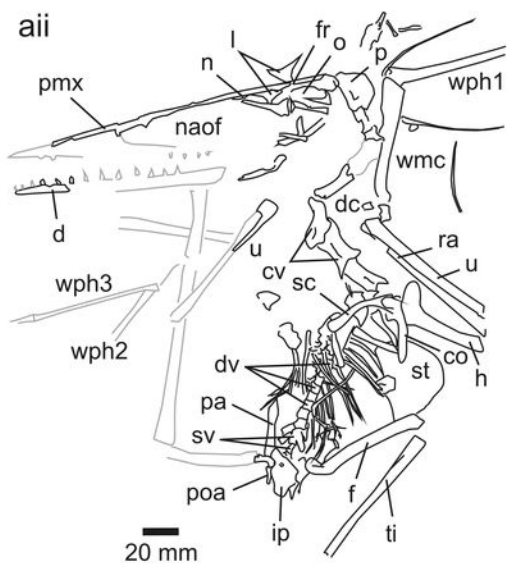
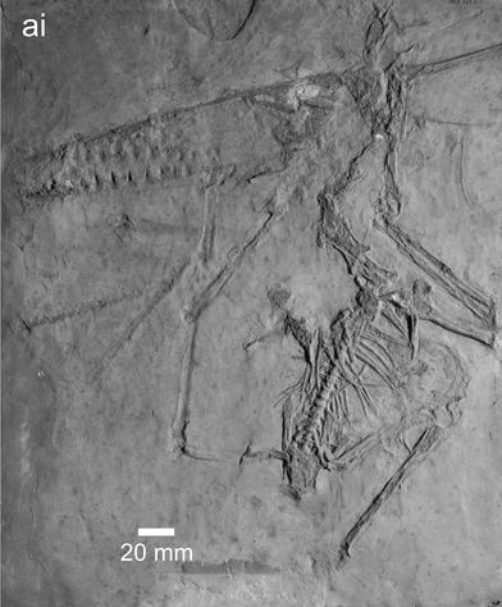
1056 referred to "*P. kochi*". (b) The cladograms of Maisch et al. (2004) and Lü et al. (2010). Note that the
1057 Lü et al. (2010) cladogram is the most parsimonious tree from the matrix, not the suboptimal tree
1058 presented in the original publication. (c) The cladogram of Lü et al. (2010) in comparison to the
1059 cladogram presented in this paper. The analyses share 53 common taxa (cii), but have many unique
1060 branches. The trees are further pruned to only the taxa in common with Maisch et al. (2004) (ci), this
1061 subtree demonstrates complete agreement.

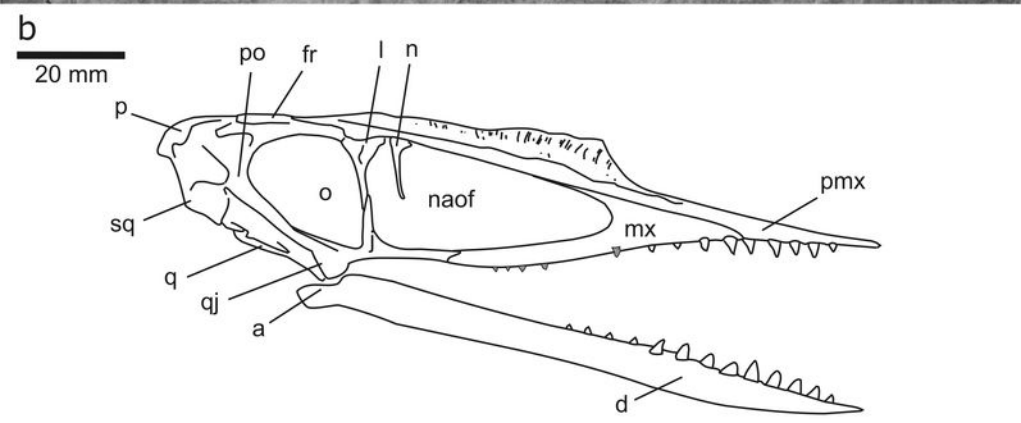
1062

1063 **Fig. 9.** Geometric morphometric dendrogram produced from a GPA of the prepubes figured. Note
1064 that a sister taxon relationship on the dendrogram means that those two species are closer to each
1065 other in prepubis morphospace than any other taxon, not that they are phyletically linked.
1066 Additionally, sister taxa in one phenetic group might be more or less morphometrically similar to
1067 each other than sister taxa in another clade. Despite the loss of information by extracting
1068 hierarchical clusters from a PCA this method is used to limit the subjectivity in interpreting the
1069 relationships observed in the PCA (see Supplementary Material). The phenetic group highlighted in
1070 dark grey consists of bi-lobed prepubes belonging to the basal-most taxa. The phenetic group
1071 highlighted in mid-grey is made up of a continuum of "transitional" taxa between the basal
1072 monofenestratans and *Germanodactylus*, typified by a robust diaphysis and broad distal expansion.
1073 The phenetic group highlighted in light grey contains the ctenochasmatooids and *Pterodactylus*,
1074 typified by a more gracile diaphysis and distal expansion.

1075 **Fig. 10.** Cranial characters and prepubes of Franconia laminated limestone pterosaurs plotted onto a
1076 pruned tree. The tree is plotted against the "fine scale" dating criteria of the Franconia laminated
1077 limestones (Schweigert, 2007). The prepubes plotted on the branches demonstrate the apomorphic
1078 and plesiomorphic conditions of the respective taxa (Fig. 9) according to the topology recovered
1079 from the cladistics analysis. The red, light blue and dark blue colours filling the prepubes indicate the
1080 phenetic groups that were found in the geometric morphometric analysis. The skulls of each taxon
1081 have arrows pointing their ventral surfaces indicating the extent of the tooth row, and arrows
1082 pointing to their dorsal surfaces indicating the extent of the premaxilla. The dashed lines represent
1083 the uncertainty of the origin of the most recent common ancestor. The red line specifies the
1084 plesiomorphic condition of the prepubis and tooth row. The yellow line specifies the gracile prepubis
1085 morphology. The blue line specifies the gracile prepubis and a dentition restricted anteriorly. The
1086 black line specifies a deep prepubis distal expansion and an edentulous jaw tip.









CLADE RETENTION INDEX (CRI)

New 1.000 0.125* 0.240* 0.244*



Maisch
et al.

1.000 0.500 0.625



Lü
et al.

0.250* 0.226*



Wang
et al.

0.391*



Andres
et al.

ROBINSON FOULDS DISTANCE (R-F)

New

0.000: 0.765: 0.633: 0.765:
0 76 62 130



Maisch et al. 0.000: 0.500: 0.667:
0 4 8



Lü et al. 0.635: 0.698:
45 70



Wang et al. 0.500:
54



Andres et al.

SPR DISTANCES

New 1.000 0.608 0.551 0.494



Maisch
et al.

1.000 0.750 0.667



Lü
et al.

0.649 0.654

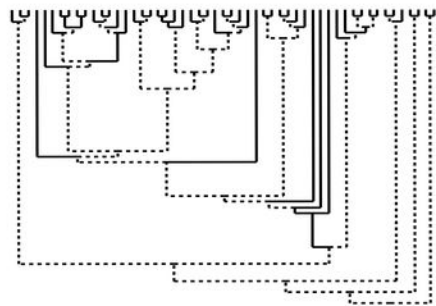
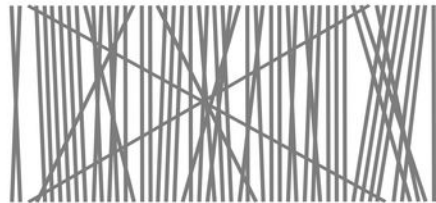
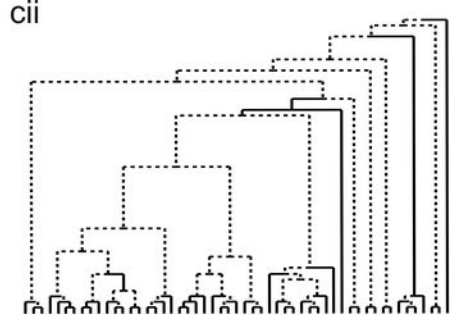
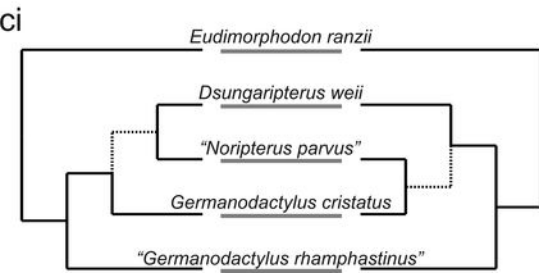
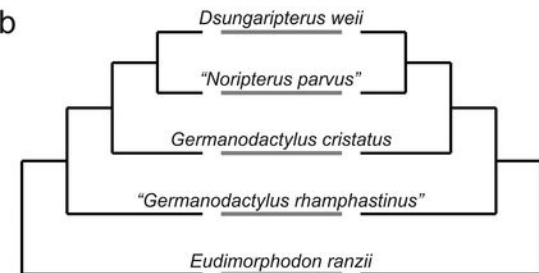
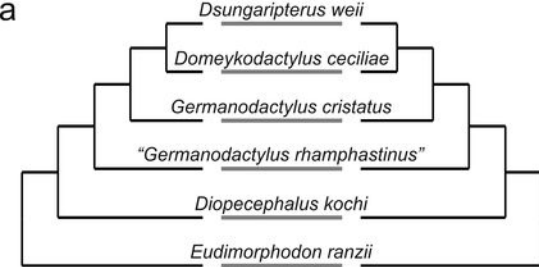


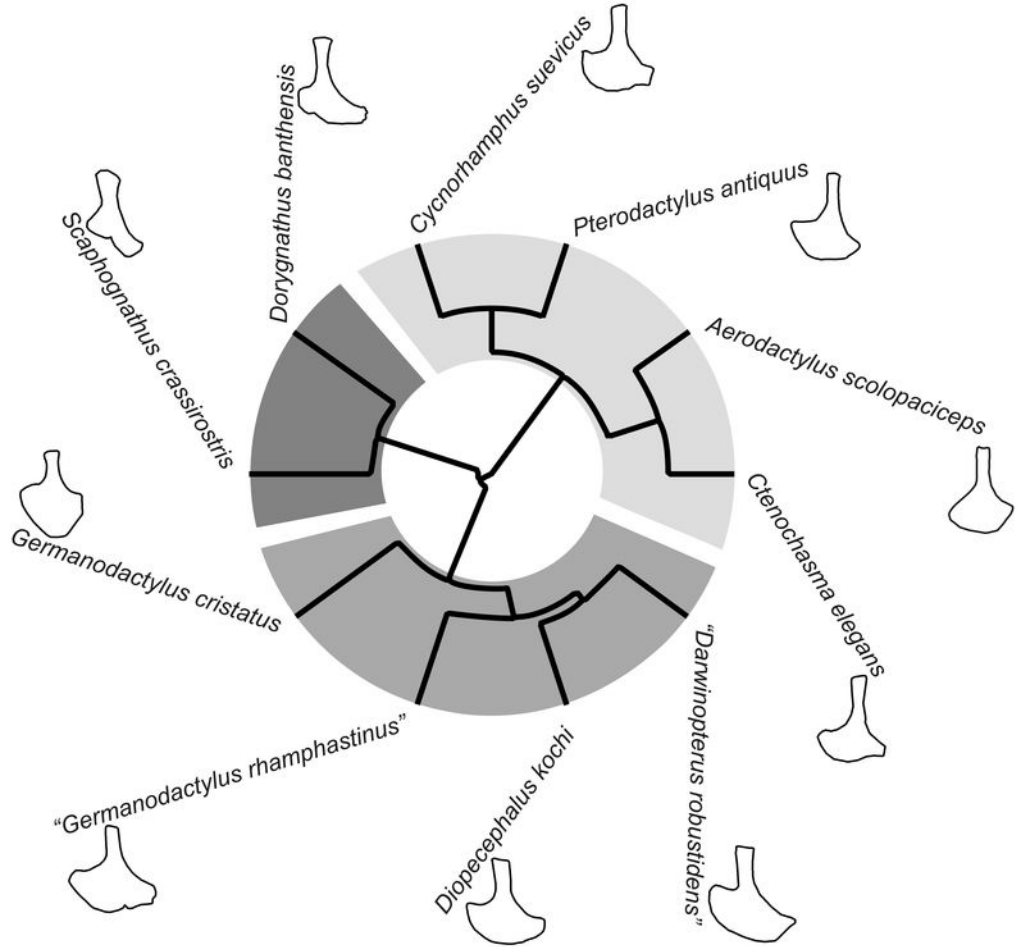
Wang
et al.

0.667



Andres
et al.





157 Ma

152 Ma

145 Ma

Oxfordian

Kimmeridgian

Tithonian

Beckeri Zone

Hybonotum Zone

Ulmense Subzone

Riedense
SubzoneRueppellianus
SubzoneMoersheimensis
Subzone